Cosmic inflation, deceleration, acceleration, dark matter, and dark 'energy' in one coherent package

Homer G. Ellis
Department of Mathematics, University of Colorado at Boulder, Boulder, Colorado 80309
(Dated: July 23, 2011)

In creating his gravitational field equations Einstein assumed without justification that inertial mass, even in its equivalent form as energy, is a source of gravity. Giving up that assumption allows modifying the field equations to a form in which a positive cosmological constant is seen to (mis)represent a uniform negative net mass density of gravitationally attractive and gravitationally repulsive matter. Field equations with both positive and negative active gravitational mass densities of both primordial and continuously created matter incorporated, along with two scalar fields to 'relax the constraints' on the space-time geometry, yield cosmological solutions that exhibit inflation, deceleration, coasting, acceleration, and a 'big bounce' instead of a 'big bang', and provide good fits to a Hubble diagram of type Ia supernovae data. The repulsive matter is identified as the back sides of the 'drainholes' introduced by the author in 1973 as solutions of those same field equations. Drainholes are topological tunnels in space which gravitationally attract on their front, entrance sides and repel more strongly on their back, exit sides. The front sides serve both as the gravitating cores of the visible, baryonic particles of primordial matter and as the continuously created, invisible particles of the 'dark matter' needed to hold together the large scale structures seen in the universe; the back sides serve as the misnamed 'dark energy' driving the current acceleration of the expansion of the universe. Formation of cosmic voids, walls, filaments, and nodes is attributed to expulsion of drainhole entrances from regions populated by drainhole exits, and accumulation of the entrances on boundaries separating those regions.

PACS numbers: PACS numbers: 98.80.Jk, 98.80.Cq, 95.35.+d, 95.36.+x

CONTENTS

I. INTRODUCTION 2

II. EINSTEIN'S UNJUSTIFIED ASSUMPTION 2

III. NEW, IMPROVED FIELD EQUATIONS 4

IV. COSMIC EVOLUTION EQUATIONS 5

V. COSMOLOGICAL SOLUTIONS 9
A. Flat open universe ($k = 0$) 9
B. Nonflat open ($k = -1$) and closed ($k = 1$) universes 11

VI. DARK MATTER AND DARK 'ENERGY' 17
A. Drainholes 17
B. Dark matter and dark 'energy' from drainholes 19

VII. ISSUES AND OBSERVATIONS 22
A. Gravity and passive-inertial mass 22
B. Choice of a variational principle for gravity 22
C. Inflation and the 'big bounce' 23
D. The PCB model vis-à-vis the ΛCDM model 23
E. Dark matter, dark 'energy', and the 'Cosmological Constant Problem' 24
F. Ratio of dark matter to baryonic matter 24
G. Continuous creation of C-matter tunnels 25
H. Voids, walls, filaments, and nodes 25
I. Geometric units and inertial mass 26
J. Protons, neutrons, and WIMPs as drainholes 26
K. Galactic nuclei as drainholes 27
L. Drainholes and Hawking radiation 28

VIII. SUMMARY 29

References 29

I. INTRODUCTION

In an article published in Journal of Mathematical Physics in 1973 I derived and analyzed in detail a model for a gravitating particle that was an improvement on the Schwarzschild blackhole model [1]. This static and spherically symmetric space-time manifold, discovered independently at about the same time by K. A. Bronnikov [2] and formally some years earlier by O. Bergmann and R. Leipnik who rejected it for "physical reasons" [3], I termed a 'drainhole' with 'ether' flowing through it. The manifold is geodesically complete, singularity-free, and devoid of horizons. It comprises a topological hole (the 'drainhole') connecting two spatial regions, an 'upper' and a 'lower', on which there is a space-time vector field (the 'ether-flow' vector field) representing the velocities of test particles free-falling from rest at infinity in the upper region, into and through the hole, and out into the lower region, accelerating downward all the way. The upper region being asymptotic to a Schwarzschild manifold with positive mass parameter m, the lower region is asymptotic to a Schwarzschild manifold with negative mass parameter $\bar{m} = -me^{m\pi/\sqrt{n^2-m^2}}$, where n is a parameter that determines the size of the hole. Thus the drainhole attracts test particles on its high side, but repels them on the low side more strongly, in the ratio $-\bar{m}/m = e^{m\pi/\sqrt{n^2-m^2}}$. The drainhole can be thought of as a kind of natural accelerator of the 'gravitational ether', drawing it in on the high side and expelling it more forcefully on the low side. To avoid ambiguities associated with the term 'ether' one could say that it is space itself that is flowing into and through the drainhole, a substitution that would accord well with Einstein's insight that the concepts of space and of a gravitational ether are essentially interchangeable [4].

In the 1973 paper I wrote that a "speculative extrapolation from the asymmetry between m and $\bar{m}$ is that the universe expands because it contains more negative mass than positive, each half-particle of positive mass m being slightly overbalanced by a half-particle of negative mass $\bar{m}$ such that $-\bar{m} > m$." This speculation lay dormant until the beginning of 2006, when it occurred to me that the same mechanism might be used to explain not only the expansion of the universe but also the recently discovered acceleration of that expansion. To properly exploit that idea I have found it necessary to reject three of the assumptions that have been built into standard relativistic cosmological theory from its earliest days. The first is Einstein's implicit assumption that active gravitational mass and passive-inertial mass are the same thing. The second, which uncritical acceptance of the first gives rise to, is that if a field thought to be associated with some form of matter couples to geometry in the field equations of space-time with the 'wrong' polarity (the 'wrong sign of the coupling constant'), then that form of matter is a 'phantom' or 'ghost' form that can exist only in 'exotic' circumstances. The third is that every scalar field included in a variational principle of relativistic gravitational theory must represent some form of matter and must therefore have its own separate field equation produced by variation of that field in the action integral of the variational principle.

As I shall show, denial of these three assumptions is logically consistent and allows one to arrive at a purely geometric theory of gravitation that produces a singularity-free cosmological model of the universe that fits with very good precision Hubble diagram data from recent observations of type Ia supernovae. This model features a 'big bounce' (instead of a 'big bang'), rapid inflation out of the bounce, and a 'graceful exit' from the inflation into a long period of decelerative coasting, followed by a transition to an ultimately exponential, de Sitter-like accelerating expansion. In addition, attributing the accelerating expansion to the existence of drainholes provides explanations for dark matter, dark 'energy', and the formation of cosmic voids, walls, filaments, and nodes. The model is offered as a replacement for and improvement on the standard ΛCDM cosmological model.

II. EINSTEIN'S UNJUSTIFIED ASSUMPTION

Albert Einstein, in his 1916 paper Die Grundlage der allgemeinen Relativitätstheorie [5] that gave a thorough presentation of the theory of gravity he had worked out over the preceding decade, made an assumption that does not hold up well under scrutiny. Stripped down to its barest form the assumption is that inertial mass, and by extension energy *via* $E = mc^2$, is a source of gravity and must therefore be coupled to the gravitational potential in the field equations of the general theory of relativity. The train of thought that brought him to this conclusion is described in §16, where he sought to extend his field equations for the vacuum, $\boldsymbol{R}_{\alpha\beta} - \frac{1}{2}\boldsymbol{R}g_{\alpha\beta} = 0$ as currently formulated, to include the contribution of a continuous distribution of gravitating matter of density ρ, in analogy to the extension of the Laplace equation $\nabla^2\phi = 0$ for the newtonian gravitational potential ϕ to the Poisson equation $\nabla^2\phi = 4\pi\kappa\rho$, where κ is Newton's gravitational constant. Einstein referred to ρ as the "density of matter", without specifying what was meant by 'matter' or its 'density'. Invoking the special theory's identification of "inert mass" with "energy, which finds its complete mathematical expression in . . . the energy-tensor", he concluded that "we must introduce a corresponding energy-tensor of matter $\mathrm{T}^{\alpha}_{\sigma}$". Further describing this energy-tensor as "corresponding to the density ρ in Poisson's equation", he arrived at the extended field equations $\boldsymbol{R}_{\alpha\beta} - \frac{1}{2}\boldsymbol{R}g_{\alpha\beta} = \frac{8\pi\kappa}{c^2}T_{\alpha\beta}$, in which, for a "frictionless adiabatic fluid" of "density" ρ, pressure p (a form of kinetic energy), and proper four-velocity distribution u^{α}, he took $T^{\alpha\beta}$ to be $\rho u^{\alpha}u^{\beta} - (p/c^2)g^{\alpha\beta}$ ([5],§19).

Clearly, Einstein's procedure fails to distinguish between the 'active gravitational mass' of matter, which measures how much gravity it produces and is the sole contributor to the "density of matter" in Poisson's equation, and the "inert mass" of matter, which measures how much it accelerates in response to forces applied to it, an effect entirely different from the production of gravity. These two conceptually different masses, along with yet a third, all occur in Newton's gravitational equation

$$m_{\rm in}\, a_{\rm B} = F_{\rm AB} = -\kappa \frac{m_{\rm pa} M_{\rm ac}}{r^2}\,, \tag{1}$$

in which $M_{\rm ac}$ is the *active* gravitational mass of a gravitating body A, $m_{\rm in}$ is the *inertial* ("inert") mass of a body B being acted upon by the gravity of A, and $m_{\rm pa}$ is the *passive* gravitational mass of B, a measure of the strength of B's 'sensing' of the gravitational field around A. That in suitable units $m_{\rm in} = m_{\rm pa}$ for all bodies is another way of saying that all bodies respond with the same accelerations to the same gravitational fields, that, in consequence, the notion of a gravitational field is more fundamental than the notion of a gravitational force. Simple thought experiments of Galileo (large stone and smaller stone tied together) [6] and Einstein (body suspended by a rope in an elevator) [7] make it clear that bodies do all respond alike — an observation now treated as a principle, the (weak) 'principle of equivalence', experimentally, if somewhat redundantly, well confirmed.

That this passive-inertial mass $m_{\text{pa-in}} = m_{\rm pa} = m_{\rm in}$ has any relation to active gravitational mass is not apparent in Eq. (1), where, unlike $m_{\rm in}$ and $m_{\rm pa}$, $M_{\rm ac}$ quantifies a property of A, not of B. But Newton's equation for the gravitational action of B on A reads

$$M_{\rm in}\, a_{\rm A} = F_{\rm BA} = -\kappa \frac{M_{\rm pa} m_{\rm ac}}{r^2}\,. \tag{2}$$

Application of Newton's law of action and reaction allows the inference that $F_{\rm AB}$ and $F_{\rm BA}$ have the same magnitude, from which follows that $m_{\rm ac}/m_{\rm pa} = M_{\rm ac}/M_{\rm pa}$, hence that the ratio of active gravitational mass to passive gravitational mass, thus to inertial mass, is the same for all bodies. It would seem likely that Einstein relied, either consciously or unconsciously, on this consequence of Newton's laws when he assumed that "inert mass" should contribute to the "density of matter" as a source of gravity in the field equations.

Newton's law of action and reaction is applicable to the bodies A and B only under the condition that gravity acts at a distance instantaneously, that is, at infinite propagation speed. But the general theory of relativity that Einstein was expounding is a field theory in which gravitational effects propagate at finite speed. Within his own theory of gravity there is, therefore, no obvious justification for Einstein's assumption that inertial mass (and therefore energy) is equivalent to active gravitational mass. This, however, is not to say that there is no relation at all between the two kinds of mass. There is, for example, the seemingly universal coincidence that wherever there is matter made of atoms there are to be found both inertial mass and active gravitational mass. Indeed, the fact that Newton's theory gives results that describe as well as they do the motions of the planets and their satellites would argue for some proportionality between $m_{\rm ac}$ and $m_{\rm pa}$ for such matter in bulk — not, however, for each individual constituent of such matter. A 1986 analysis of lunar data concluded that the ratio of $m_{\rm ac}$ to $m_{\rm pa}$ for aluminum differs from that for iron by less than 4×10^{-12} [8]. An earlier, Cavendish-balance experiment had put a limit of 5×10^{-5} on the difference of these ratios for bromine and fluorine [9]. But those results are only for matter in bulk, that is, matter made of atoms and molecules. It is entirely possible that electrons, for example, do not gravitate at all, for no one has ever established by direct observation that they do, nor is it likely that anyone will. There is in the literature an argument that purports to show that if the ratio $m_{\rm ac}/m_{\rm pa}$ is the same for two species of bulk matter, then electrons must be generators of gravity [10], but that argument can be seen on careful examination to rest on an unrecognized, hidden assumption of its own, namely that, in simplest form, the gravitational field of a hydrogen atom at a distance could be distinguished from that of a neutron at the same distance [11] — another assumption no one has tested or is likely to test by direct observation.

Einstein's assumption that energy and inertial mass are sources of gravity has survived to the present virtually unchallenged.[1] It has generated a number of consequences that have directed much of the subsequent research in gravitation theory — indeed, misdirected it if his assumption is wrong. Among them are the following:

- The impossibility, according to Penrose–Hawking singularity theorems, of avoiding singularities in the geometry of space-time without invoking 'negative energy', which is really just energy coupled to gravity with polarity opposite to that of the coupling of matter to gravity.
- The presumption that the extra, fifth dimension in Kaluza–Klein theory must be a spatial dimension rather than a dimension of another type.

[1] Curiously, Herman Bondi in a paper in 1957 carefully distinguished between passive-inertial mass and active mass, then in the same paper adopted Einstein's "energy-tensor" which ignores the distinction [12].

- The belief that all the extra dimensions in higher-dimensional theories must be spatial, causing the expenditure of much effort in mental gymnastics to explain why they are not apparent to our senses in the way that the familiar three spatial dimensions are.

Denying Einstein's assumption relieves one of the burden of these troublesome conclusions and opens the door to other, more realistic ones.

III. NEW, IMPROVED FIELD EQUATIONS

If Einstein's assumption is to be disallowed, then his source tensor for a continuous distribution of gravitating matter, $T^{\alpha\beta} = \rho u^\alpha u^\beta - (p/c^2) g^{\alpha\beta}$, must be modified or replaced. One might think simply to drop the pressure term and take $T^{\alpha\beta} = \rho u^\alpha u^\beta$, the energy-momentum tensor of the matter. This would be inconsistent, for the ρ in that tensor is the density of inertial mass, which we are now not assuming to be the same as active gravitational mass. What to do instead?

At the same time that Einstein was creating his field equations David Hilbert was deriving the field equations for (in particular) empty space from the variational principle $\delta \int \boldsymbol{R}\, |g|^{\frac{1}{2}} d^4x = 0$ [13]. This is the most straightforward extension to the general relativity setting of the variational principle $\delta \int |\nabla\phi|^2\, d^3x = 0$, whose Euler–Lagrange equation is equivalent to the Laplace equation $\nabla^2\phi = 0$ for the newtonian potential ϕ. Modifying that principle to $\delta \int (|\nabla\phi|^2 + 8\pi\kappa\mu\phi)\, d^3x = 0$, where μ is the density of the *active* gravitational mass of matter, generates the Poisson equation $\nabla^2\phi = 4\pi\kappa\mu$. The most straightforward extension of this modified principle to general relativity is

$$\delta \int (\boldsymbol{R} - \tfrac{8\pi\kappa}{c^2}\mu)\, |g|^{\frac{1}{2}} d^4x = 0\,, \tag{3}$$

for which the Euler–Lagrange equations are equivalent to

$$\boldsymbol{R}_{\alpha\beta} - \tfrac{1}{2}\boldsymbol{R}\, g_{\alpha\beta} = -\tfrac{4\pi\kappa}{c^2}\mu g_{\alpha\beta}\,, \tag{4}$$

which makes $T_{\alpha\beta} = -\frac{1}{2}\mu g_{\alpha\beta}$. Equivalent to this equation is $\boldsymbol{R}_{\alpha\beta} = \frac{4\pi\kappa}{c^2}\mu g_{\alpha\beta}$, the 00 component of which reduces in the slowly varying, weak field approximation to the Poisson equation, with $\phi = \frac{1}{2}(g_{00} - c^2)$.

The vanishing of the divergence of the Einstein tensor field on the lefthand side of Eq. (4) entails that $0 = T_\alpha{}^\beta{}_{:\beta} = -\frac{1}{2}(\mu_{.\beta} g_\alpha{}^\beta + \mu g_\alpha{}^\beta{}_{:\beta}) = -\frac{1}{2}\mu_{.\alpha}$, hence that μ is a constant. This would seem to be a comedown from the equations of motion of the matter distribution implied by the vanishing of the divergence of Einstein's $T^{\alpha\beta}$, but those equations are unrealistic in that they have the density ρ of inertial mass playing a role that would properly belong to the density μ of active mass in any such equations derived from *gravitational* field equations. As will be seen, the new, improved field equations to be arrived at will allow μ to vary.

To widen the range of space-time geometries admitted by the field equations one can in the usual way add to the action integrand of Eq. (3) terms related to such things as scalar fields and electromagnetic fields. In particular, one can add a cosmological constant term, changing the integrand to $\boldsymbol{R} - \frac{8\pi\kappa}{c^2}\mu + 2\Lambda$ and the field equations to

$$\boldsymbol{R}_{\alpha\beta} - \tfrac{1}{2}\boldsymbol{R}\, g_{\alpha\beta} = -\tfrac{4\pi\kappa}{c^2}\mu\, g_{\alpha\beta} + \Lambda\, g_{\alpha\beta} = -\tfrac{4\pi\kappa}{c^2}(\mu + \bar{\mu})\, g_{\alpha\beta}\,, \tag{5}$$

where $\bar{\mu} = -\frac{c^2}{4\pi\kappa}\Lambda$. A positive cosmological constant Λ thus appears in this context to be a (mis)representation of a negative active mass density $\bar{\mu}$ of a continuous distribution of gravitationally repulsive matter. The same field equations are obtained by changing the integrand to $\boldsymbol{R} + 2\Lambda$ and setting $\Lambda = -\frac{4\pi\kappa}{c^2}(\mu + \bar{\mu})$, thus associating a positive Λ with a negative *net* active mass density of gravitating matter, some attractive, some repulsive. As suggested in the Introduction, an excess of the negative active mass density $\bar{\mu}$ of repulsive matter over the positive density μ of attractive matter could drive an accelerating cosmic expansion (and in the process would solve the vexing 'Cosmological Constant Problem' by identifying $-\frac{c^2}{4\pi\kappa}\Lambda$ as the net density $\mu + \bar{\mu}$ of gravitating matter). Leaving for later a full discussion of drainholes as the source of such a density imbalance (cf. Sec. VI.A), let us explore the consequences of an imbalance by studying cosmological solutions of field equations that incorporate a positive mass density μ, a negative mass density $\bar{\mu}$, and scalar fields ϕ (not the newtonian ϕ) and ψ, all coupled to the space-time geometry *via* the variational principle

$$\delta \int [\boldsymbol{R} - \tfrac{8\pi\kappa}{c^2}(\mu + \bar{\mu}) + 2\,\phi^{\cdot\gamma}\phi_{.\gamma} - 2\,\psi^{\cdot\gamma}\psi_{.\gamma}]\, |g|^{\frac{1}{2}} d^4x = 0\,. \tag{6}$$

In deriving field equations from this variational principle I will vary only the space-time metric. Not varying the densities is normal, but not varying the scalar fields goes against orthodox practice. The rationale for leaving them

unvaried is this: In a space-time manifold the geometry is determined by the metric alone, so only the metric should participate in the extremizing of the action; to vary the scalar fields would be to treat them as something extraneous to the metric thus to the geometry, whereas their proper role should be simply to introduce a useful flexibility into the extremizing process, *not* to represent explicit contributions to gravity by the 'energy' fields of distributions of scalar matter. Varying neither the scalar fields nor the densities, but only the metric, is in keeping with Einstein's guiding principle that geometry can explain all of physics.

Looked at another way, including the terms $-\frac{8\pi\kappa}{c^2}\mu$, $-\frac{8\pi\kappa}{c^2}\bar{\mu}$, $2\,\phi^{\cdot\gamma}\phi_{.\gamma}$, and $-2\,\psi^{\cdot\gamma}\psi_{.\gamma}$ in the action can be seen as allowing 'relaxations' of the metric, analogously to accommodating 'constraints' on the metric by including Lagrange multipliers in the action (e. g., λ in the action $\int(\boldsymbol{R}+\lambda)\,|g|^{\frac{1}{2}}d^nx = \int \boldsymbol{R}\,|g|^{\frac{1}{2}}d^nx + \lambda\int|g|^{\frac{1}{2}}d^nx$ for an n-dimensional Einstein manifold, to accommodate the constraint that the volume $\int|g|^{\frac{1}{2}}d^nx$ of the integration region is held fixed). Just as one does not vary Lagrange multipliers, one should not vary μ, $\bar{\mu}$, ϕ, or ψ. In this role μ, $\bar{\mu}$, ϕ, and ψ simply relax the field equations to allow a larger class of metrics to satisfy them. The relaxed field equations will be as useful as the metrics that satisfy them, no more, no less.

Breaking the scalar field portion of the action into two parts, one ($2\,\psi^{\cdot\gamma}\psi_{.\gamma}$) coupled to geometry with the orthodox polarity, the other ($2\,\phi^{\cdot\gamma}\phi_{.\gamma}$) coupled with the opposite ('phantom' or 'ghost') polarity is justified by the absence of any compelling reason for choosing one coupling over the other. The usual mantra accompanying the making of such a choice is that a scalar field coupled to geometry with the 'wrong sign' has 'negative energy' and therefore represents 'exotic matter' that can exist if at all only in highly contrived circumstances. This superstition traces back to Einstein's mistaking as active the passive-inertial density ρ in his "energy-tensor of matter $\mathrm{T}^{\alpha}_{\sigma}$". If his field equations $\boldsymbol{R}_{\alpha\beta} - \frac{1}{2}\boldsymbol{R}g_{\alpha\beta} = \frac{8\pi\kappa}{c^2}T_{\alpha\beta}$ were changed to $\boldsymbol{R}_{\alpha\beta} - \frac{1}{2}\boldsymbol{R}g_{\alpha\beta} = -\frac{8\pi\kappa}{c^2}T_{\alpha\beta}$, the effect, in the absence of pressure, would be equivalent to taking the density ρ to be negative in the original equations, in which case the matter it purports to represent would be gravitationally repulsive, and 'exotic' for having negative inertial mass and therefore negative energy. Correcting this mistake reveals the constructions 'exotic matter with negative energy density', 'phantom field', 'ghost field', and others like them to be little more than instances of misleading jargon.

Variation of the metric in the action integral of Eq. (6) generates the field equations

$$\boldsymbol{R}_{\alpha\beta} - \tfrac{1}{2}\boldsymbol{R}\,g_{\alpha\beta} = \tfrac{8\pi\kappa}{c^2}T_{\alpha\beta} \coloneqq -\tfrac{4\pi\kappa}{c^2}(\mu+\bar{\mu})\,g_{\alpha\beta} - 2\,(\phi_{.\alpha}\phi_{.\beta} - \tfrac{1}{2}\phi^{\cdot\gamma}\phi_{.\gamma}\,g_{\alpha\beta}) + 2\,(\psi_{.\alpha}\psi_{.\beta} - \tfrac{1}{2}\psi^{\cdot\gamma}\psi_{.\gamma}\,g_{\alpha\beta})\,, \tag{7}$$

and

$$2\,(\Box\phi)\phi_{.\alpha} - 2\,(\Box\psi)\psi_{.\alpha} \coloneqq 2\,\phi^{\cdot\gamma}{}_{;\gamma}\phi_{.\alpha} - 2\,\psi^{\cdot\gamma}{}_{;\gamma}\psi_{.\alpha} = -\tfrac{4\pi\kappa}{c^2}(\mu+\bar{\mu})_{.\alpha}\,. \tag{8}$$

The latter of these, which follows from the vanishing of the divergence of $\boldsymbol{R}_{\alpha\beta} - \frac{1}{2}\boldsymbol{R}\,g_{\alpha\beta}$ in the former, is what one has in place of the wave equations $\Box\phi = 0$ and $\Box\psi = 0$ that would have resulted from varying ϕ and ψ. It leaves ϕ and ψ underdetermined, which is consistent with their roles as 'relaxants' to allow a wider range of metrics to satisfy the field equations than would be allowed in their absence.

IV. COSMIC EVOLUTION EQUATIONS

For a Robertson–Walker metric $c^2dt^2 - R^2(t)ds^2$ (with t in seconds, s dimensionless, c in centimeters per second, and R in centimeters) and dimensionless scalar fields $\phi = \alpha(t)$ and $\psi = \beta(t)$ the field equations (7) reduce to

$$3\,\frac{\dot{R}^2/c^2 + k}{R^2} = -\frac{4\pi\kappa}{c^2}(\mu+\bar{\mu}) - \frac{\dot{\alpha}^2 - \dot{\beta}^2}{c^2}\,, \tag{9}$$

and

$$\frac{2}{c^2}\frac{\ddot{R}}{R} + \frac{\dot{R}^2/c^2 + k}{R^2} = -\frac{4\pi\kappa}{c^2}(\mu+\bar{\mu}) + \frac{\dot{\alpha}^2 - \dot{\beta}^2}{c^2}\,, \tag{10}$$

where $k = -1$, 0, or 1, the uniform curvature of the spatial metric ds^2. These equations, which are replacements for the well-studied Friedmann–Lemaître cosmological equations, are equivalent together to

$$\frac{1}{c^2}\frac{\dot{R}^2}{R^2} = -\frac{4\pi\kappa}{3c^2}(\mu+\bar{\mu}) - \frac{k}{R^2} - \frac{\dot{\alpha}^2 - \dot{\beta}^2}{3c^2} \tag{11}$$

and

$$\frac{1}{c^2}\frac{\ddot{R}}{R} = -\frac{4\pi\kappa}{3c^2}(\mu+\bar{\mu}) + \frac{2(\dot{\alpha}^2 - \dot{\beta}^2)}{3c^2}\,. \tag{12}$$

Equations (8) reduce to

$$\frac{2}{c^2}\left(\ddot{\alpha}+3\,\frac{\dot{R}}{R}\dot{\alpha}\right)\dot{\alpha}-\frac{2}{c^2}\left(\ddot{\beta}+3\,\frac{\dot{R}}{R}\dot{\beta}\right)\dot{\beta}=-\frac{4\pi\kappa}{c^2}\partial_t(\mu+\bar{\mu}) \tag{13}$$

for the time component and $\partial_\alpha(\mu+\bar{\mu})=0$ for the space components, thus impose spatial but not temporal uniformity on $\mu+\bar{\mu}$. Equation (13) is equivalent to

$$\frac{1}{c^2}\left(R^6(\dot{\alpha}^2-\dot{\beta}^2)\right)^{\cdot}=-\frac{4\pi\kappa}{c^2}R^6\partial_t(\mu+\bar{\mu})\,. \tag{14}$$

To give substance to the densities μ and $\bar{\mu}$, let us invoke two kinds of gravitating matter: a) *primordial matter*, existent at all times, never changing in amount, with its net density $\mu+\bar{\mu}$ inversely proportional to the cube of the scale factor R; and b) *continuously created* (or *destroyed*) *matter*, coming steadily into existence (or passing out of existence) at a rate just sufficient to keep its net density constant. For primordial matter we have

$$\mu_{\rm P}(t)+\bar{\mu}_{\rm P}(t)=(\mu_{\rm P,0}+\bar{\mu}_{\rm P,0})\frac{R^3(t_0)}{R^3(t)}\,, \tag{15}$$

where t_0 denotes the value of t at the present epoch, and $\mu_{\rm P,0}$ and $\bar{\mu}_{\rm P,0}$ are the present values of the primordial densities $\mu_{\rm P}$ and $\bar{\mu}_{\rm P}$. For continuously created matter we have

$$\mu_{\rm C}(t)+\bar{\mu}_{\rm C}(t)=\mu_{\rm C,0}+\bar{\mu}_{\rm C,0}\,, \tag{16}$$

where $\mu_{\rm C,0}$ and $\bar{\mu}_{\rm C,0}$ are the present values of the continuously created densities $\mu_{\rm C}$ and $\bar{\mu}_{\rm C}$. Under the assumption that the net densities $\mu_{\rm P}+\bar{\mu}_{\rm P}$ and $\mu_{\rm C}+\bar{\mu}_{\rm C}$ are additive, Eq. (14) turns into

$$\frac{1}{c^2}\Big(R^6(\dot{\alpha}^2-\dot{\beta}^2)\Big)^{\cdot}=\frac{4\pi\kappa}{c^2}(\mu_{\rm P,0}+\bar{\mu}_{\rm P,0})\,R^3(t_0)\left(R^3\right)^{\cdot}\,, \tag{17}$$

which integrates to

$$\frac{1}{c^2}(\dot{\alpha}^2-\dot{\beta}^2)=\frac{4\pi\kappa}{c^2}(\mu_{\rm P,0}+\bar{\mu}_{\rm P,0})\frac{R^3(t_0)}{R^3}+\frac{B}{R^6}\,, \tag{18}$$

where B is the constant of integration, with units cm^4.

At this point it is convenient to set

$$A_{\rm P}:=-\frac{4\pi\kappa}{c^2}(\mu_{\rm P,0}+\bar{\mu}_{\rm P,0})\,R^3(t_0) \tag{19}$$

(units cm) and

$$A_{\rm C}:=-\frac{4\pi\kappa}{c^2}(\mu_{\rm C,0}+\bar{\mu}_{\rm C,0}) \tag{20}$$

(units cm^{-2}). Equation (18) then becomes

$$\frac{1}{c^2}(\dot{\alpha}^2-\dot{\beta}^2)=\frac{B-A_{\rm P}R^3}{R^6}\,, \tag{21}$$

and substitution from Eqs. (19), (20), and (21) into Eqs. (11) and (12) produces

$$\frac{1}{c^2}\frac{\dot{R}^2}{R^2}=\frac{P_1(R)}{3R^6}=\frac{A_{\rm C}}{3}-\frac{k}{R^2}+\frac{2A_{\rm P}}{3R^3}-\frac{B}{3R^6} \tag{22}$$

and

$$\frac{1}{c^2}\frac{\ddot{R}}{R}=\frac{P_2(R)}{3R^6}=\frac{A_{\rm C}}{3}-\frac{A_{\rm P}}{3R^3}+\frac{2B}{3R^6}\,, \tag{23}$$

where

$$P_1(R) := A_{\mathrm{C}}R^6 - 3kR^4 + 2A_{\mathrm{P}}R^3 - B \tag{24}$$

and

$$P_2(R) := A_{\mathrm{C}}R^6 - A_{\mathrm{P}}R^3 + 2B\,. \tag{25}$$

According to Eqs. (19) and (20), positive values for A_{P} and A_{C} correspond to negative net densities for primordial matter and continuously created matter, signifying that on balance each kind gravitationally repels all other matter more strongly than it attracts other matter. This excess of repulsion over attraction will be presumed to exist for both types. With thus $A_{\mathrm{P}} > 0$ and $A_{\mathrm{C}} > 0$ assumed, along with an added assumption that $B > 0$, several properties of the scale factor R as a solution of these equations can be inferred rather easily, to wit:

- For each of $k = -1$, 0, 1 there is a least positive number $R_{\min}$ (the least positive root of the polynomial $P_1(R)$) that R cannot go below without violating Eq. (22), and at which $\dot{R} = 0$. (See Fig. 1.) This sets a positive lower bound on the compression of space and thereby rules out the development of a 'big bang' singularity.

- For $k = 1$ and some choices of A_{C}, A_{P}, and B (Fig. 1, graphs b, c, and d) there are in addition to $R_{\min}$ other values $R_{\max}$ and $R_{\min *}$ of R at which P_1, and consequently $\dot{R}$, vanish.

- The identity $P_2(R) = \frac{1}{2}RP_1'(R) - 2P_1(R)$ has the consequence that because, with one exception (Fig. 1, graph b), $P_1'(R_{\min}) > 0$, also $P_2(R_{\min}) > 0$, and therefore $\ddot{R}$ is positive when $R = R_{\min}$. This tells that in place of a 'big bang' there is a 'bounce' off a state of maximum compression at the time when $R = R_{\min}$. The lone exception has $k = 1$, $P_2(R_{\min}) = P_1'(R_{\min}) = 0$, and $R(t) = R_{\min} = R_{\max}$ for all time, modeling a static, spherical universe of radius $R_{\min}$.

- With the time $t = 0$ chosen so that $R(0) = R_{\min}$, $R(t)$ is symmetric about $t = 0$, the evolution of the universe after time zero thus being mirrored in reverse as a devolution of the universe before time zero.

- Whereas for $k = -1$ and $k = 0$ (Fig. 1), and $k = 1$ (Fig. 1, graph a), the universe expands from $R_{\min}$ to infinity as $t \to \pm\infty$, other behaviors are possible when $k = 1$, most notably: (Fig. 1, graph b) static spherical universe as noted above; (Fig. 1, graph c) spherical universe oscillating for all time between minimum radius $R_{\min}$ and maximum radius $R_{\max}$.

- The polynomial $P_2(R)$ is quadratic in R^3, with discriminant $A_{\mathrm{P}}^2 - 8A_{\mathrm{C}}B$. If $B > A_{\mathrm{P}}^2/8A_{\mathrm{C}}$, then $P_2(R)$ has no positive root, so $\ddot{R} > 0$ at all times, thus the universal expansion described by $R(t)$ for times after $t = 0$ is always accelerating. If $B = A_{\mathrm{P}}^2/8A_{\mathrm{C}}$, then $P_2(R) = A_{\mathrm{C}}(R^3 - A_{\mathrm{P}}/2A_{\mathrm{C}})^2$, so the expansion is, except for a momentary pause when $R(t)$ passes through $\sqrt[3]{A_{\mathrm{P}}/2A_{\mathrm{C}}}$, accelerating at all positive times, unless, as in Fig. 1, graph b, $R(t) = R_{\min} = R_{\max}$ or, as in Fig. 1, graph d, $R(t) = R_{\max} = R_{\min *}$. If $B < A_{\mathrm{P}}^2/8A_{\mathrm{C}}$, then $P_2(R)$ has two positive roots,

$$R_{\mathrm{d}} := \left(\frac{A_{\mathrm{P}}}{2A_{\mathrm{C}}} - \frac{\sqrt{A_{\mathrm{P}}^2 - 8A_{\mathrm{C}}B}}{2A_{\mathrm{C}}}\right)^{\frac{1}{3}}, \tag{26}$$

  which marks a transition from the initial accelerating expansion associated with the bounce at $t = 0$ to an interval of decelerating expansion, and

$$R_{\mathrm{a}} := \left(\frac{A_{\mathrm{P}}}{2A_{\mathrm{C}}} + \frac{\sqrt{A_{\mathrm{P}}^2 - 8A_{\mathrm{C}}B}}{2A_{\mathrm{C}}}\right)^{\frac{1}{3}}, \tag{27}$$

  which marks a return to accelerating expansion (if the expansion is destined to continue forever, as opposed to some of the other possible behaviors when $k = 1$).

- For the infinitely expanding models the 'Hubble parameter' H and the 'acceleration parameter' Q behave asymptotically as follows:

$$H := \dot{R}/R, \qquad \frac{1}{c^2}H^2 = \frac{A_{\mathrm{C}}}{3} - \frac{3kR^4 - 2A_{\mathrm{P}}R^3 + B}{3R^6} \to \frac{A_{\mathrm{C}}}{3} \qquad \left\{\begin{matrix}\text{from below if } k > 0\\ \text{from above if } k \le 0\end{matrix}\right\} \text{ as } R \to \infty\,, \tag{28}$$

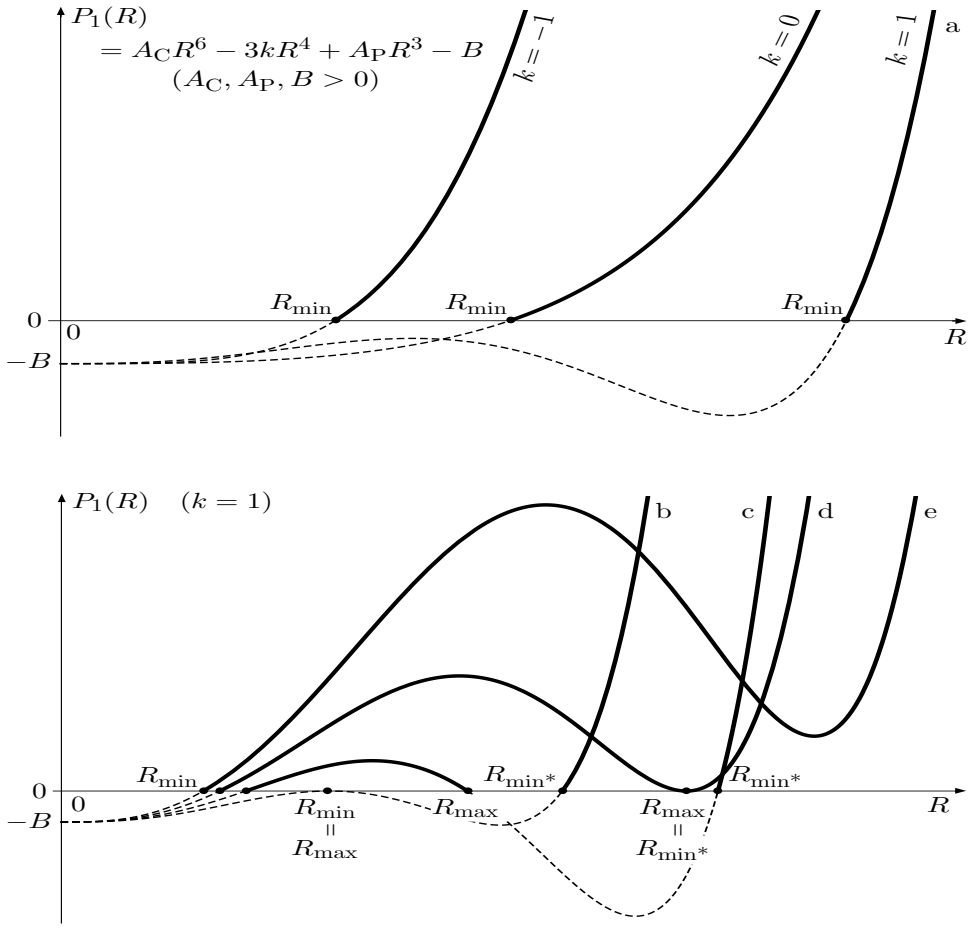

FIG. 1. Graphs of $P_1(R)$ for $k = -1$, 0, and 1, and generic positive values of the parameters A_C, A_P, and B. Values of R for which $P_1(R) < 0$ are excluded from the range of $R(t)$ by Eq. (22).

and

$$Q := \frac{\ddot{R}/R}{(\dot{R}/R)^2} = \frac{P_2(R)}{P_1(R)} = c^2\,\frac{A_C R^6 - A_P R^3 + 2B}{3H^2R^6} \tag{29}$$

$$= 1 + c^2\,\frac{kR^4 - A_P R^3 + B}{H^2R^6} \to 1 \qquad \left.\begin{matrix}\text{from above if } k > 0\\ \text{from below if } k \le 0\end{matrix}\right\} \text{ as } R \to \infty\,. \tag{30}$$

Either of these entails that, in case R has no upper bound, $R(t) \sim Ce^{\pm\sqrt{A_C/3}\,c\,t}$, for some constant C, as $t \to \pm\infty$.

- For $k = -1$ or 0, and for some cases of $k = 1$, H has a maximum value H_{max} at $R = R_{H_{max}}$, where $dH/dR = c^2(kR^4 - A_P R^3 + B)/HR^7 = 0$. If $k = 0$, $R_{H_{max}} = \sqrt[3]{B/A_P}$ and $H_{max} = c\sqrt{A_C/3 + A_P^2/3B}$. As seen in Fig. 2, H rises sharply from 0 at R_{min} to H_{max} at $R_{H_{max}}$, then reverses and tails off asymptotically to $c\sqrt{A_C/3}$. One can show that $R_{min} \sim \sqrt[3]{B/2A_P}$, $R_{H_{max}} \sim \sqrt[3]{B/A_P}$, $R_d \sim \sqrt[3]{2B/A_P}$, and $H_{max} \sim c\,A_P/\sqrt{3B}$, as $B \to 0$ with A_C and A_P fixed. Thus, as $B \to 0$ with A_C and A_P fixed, R_{min}, $R_{H_{max}}$, and R_d are squeezed together closer and closer to 0, and H_{max} grows without bound. This clearly is a recipe for an explosive postbounce inflation ending with a 'graceful exit' initiated by the onset of deceleration when R reaches R_d.

- As Fig. 2 exhibits, for $k = -1$, $k = 0$, and $k = 1$, graph a, the acceleration parameter Q, descending from ∞ at R_{min}, passes through 1 at $R_{H_{max}}$, bottoms out with a minimum value Q_{min} at $R_{Q_{min}}$, where $dQ/dR = 0$,

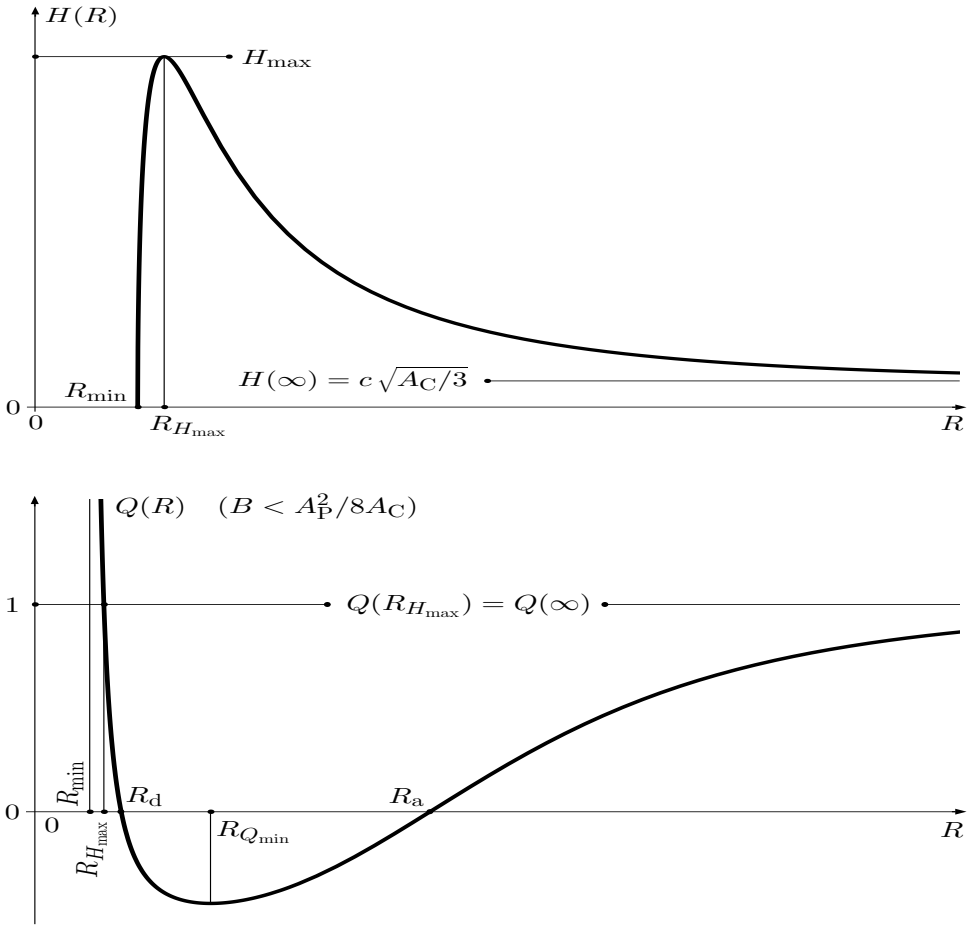

FIG. 2. Graphs of $H(R)$ and $Q(R)$ for $k = -1$ or 0 and generic positive values of the parameters $A_{\rm C}$, $A_{\rm P}$, and B, and for some cases of $k = 1$, showing early stage inflation followed by a decline in H to its asymptotic limit $H(\infty) = c\sqrt{A_{\rm C}/3}$, and (for $B < A_{\rm P}^2/8A_{\rm C}$) transitions of Q from inflationary acceleration to deceleration at $R_{\rm d}$ and back to acceleration at $R_{\rm a}$ to the asymptotic limit $Q(\infty) = 1$.

then creeps slowly back to 1 as $R \to \infty$ (with a late pass through 1 if $k = 1$). When $k = 0$, $Q_{\rm min} = -\frac{1}{2} + \frac{3}{2}\sqrt{A_{\rm C}B/(A_{\rm P}^2 + A_{\rm C}B)}$ at $R_{Q_{\rm min}} = \left(B/A_{\rm P} + \sqrt{B^2/A_{\rm P}^2 + B/A_{\rm C}}\right)^{\frac{1}{3}}$, which, with $A_{\rm C}$ and $A_{\rm P}$ fixed, are asymptotic respectively to $-\frac{1}{2}$ and $\sqrt[6]{B/A_{\rm C}}$ as $B \to 0$.

- If $k = 1$ and $A_{\rm C}$, $A_{\rm P}$, and B are such as to generate graph c of Fig. 1, then for the section bounded by $R_{\rm min}$ and $R_{\rm max}$ the behavior of R is cyclical, as Fig. 3 portrays graphically.

V. COSMOLOGICAL SOLUTIONS

A. Flat open universe ($k = 0$)

When $k = 0$, so that space is perfectly flat, $R_{\rm min}^3 = -A_{\rm P}/A_{\rm C} + \sqrt{A_{\rm P}^2 + A_{\rm C}B}/A_{\rm C}$ and it is straightforward to integrate Eqs. (22) and (23) ((23) is equivalent to a readily integrable equation linear in R^3; (22) is essentially redundant), the result being

$$R^3(t) = \left(R_{\rm min}^3 + \frac{A_{\rm P}}{A_{\rm C}}\right)\cosh\left(\sqrt{3A_{\rm C}}\,c\,t\right) - \frac{A_{\rm P}}{A_{\rm C}}\,. \tag{31}$$

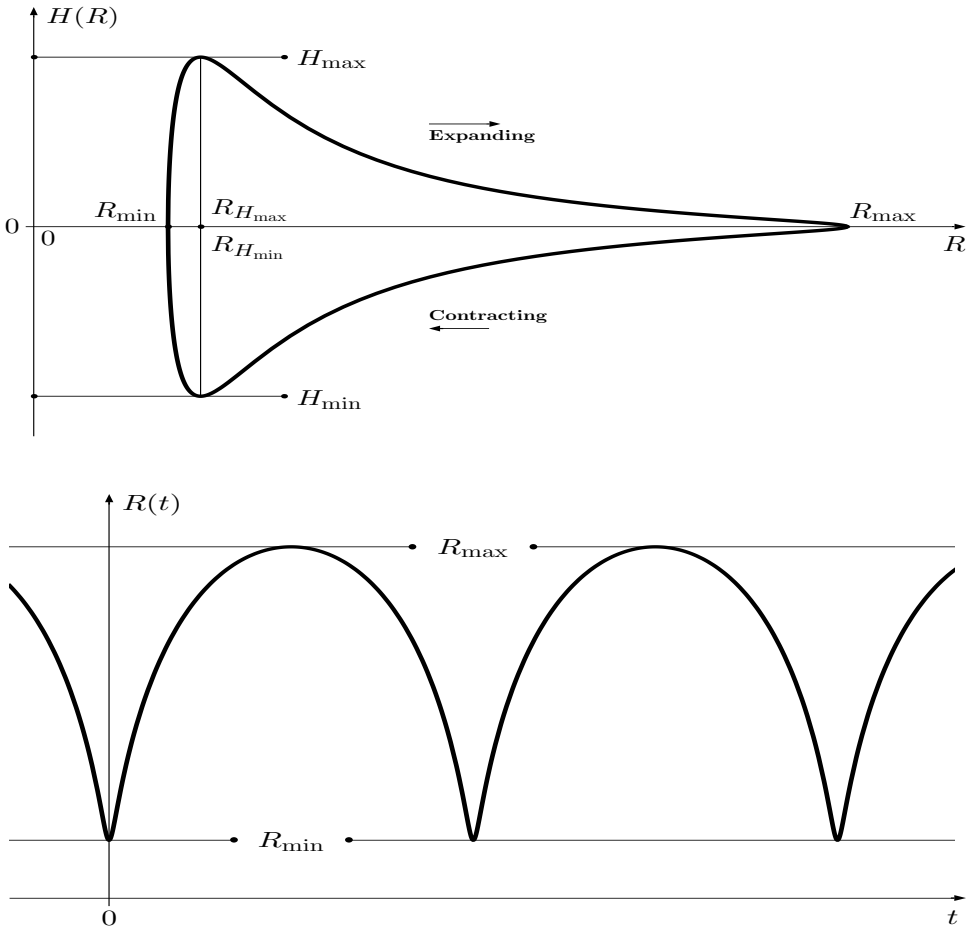

FIG. 3. Graphs of $H(R)$ and $R(t)$ for $k = 1$ and generic positive values of the parameters $A_{\rm C}$, $A_{\rm P}$, and B associated with graph c of Fig. 1, showing repetitive, identical periods of expansion and contraction, each beginning with a stage of rapid inflation from a bounce at $R = R_{\rm min}$, which is followed by a less rapid expansion to $R = R_{\rm max}$, then a mirror-image contraction to an ending stage of rapid deflation into the next bounce at $R = R_{\rm min}$. The graphed functions are related by $\dot{R}(t)/R(t) =: H(R(t))$.

One can show that if $B \leq A_{\rm P}^2/8A_{\rm C}$, so that $R_{\rm d}$ and $R_{\rm a}$ exist, then $R_{\rm min} < R_{\rm d} \leq R_{\rm a}$. The postbounce times $t_{\rm d}$ and $t_{\rm a}$ at which $R = R_{\rm d}$ and $R = R_{\rm a}$ are the positive solutions of

$$\cosh\left(\sqrt{3A_{\rm C}}\, c\, t\right) = \frac{R_{\{\rm d,a\}}^3 + A_{\rm P}/A_{\rm C}}{R_{\rm min}^3 + A_{\rm P}/A_{\rm C}}\,. \tag{32}$$

The first graph in Fig. 4 displays the evolution of $R(t)$ for generic values of $A_{\rm C}$, $A_{\rm P}$, and B with $B < A_{\rm P}^2/8A_{\rm C}$, showing the acceleration during the interval from $t = 0$ to $t = t_{\rm d}$, the deceleration during the interval from $t_{\rm d}$ to $t_{\rm a}$, and the ultimately exponential acceleration after $t_{\rm a}$.

For times $t \approx 0$, Eq. (31) yields the approximation

$$R^3(t) \approx R_{\rm min}^3 \left(1 + \frac{3A_{\rm C}}{2}\frac{R_{\rm min}^3 + A_{\rm P}/A_{\rm C}}{R_{\rm min}^3} c^2 t^2\right)\,, \tag{33}$$

which produces the further approximation that

$$R(t) \approx \hat{R}(t) \coloneqq R_{\rm min} + \frac{A_{\rm C}}{2}\left(R_{\rm min} + \frac{A_{\rm P}}{A_{\rm C}}\frac{1}{R_{\rm min}^2}\right) c^2 t^2\,, \tag{34}$$

thus that $R(t)$ is approximately parabolic, opening upward from a vertex at $R_{\rm min}$, with an inflationary 'steepness' factor that grows as $c^2 A_{\rm P}/2R_{\rm min}^2$ as $R_{\rm min} \to 0$.

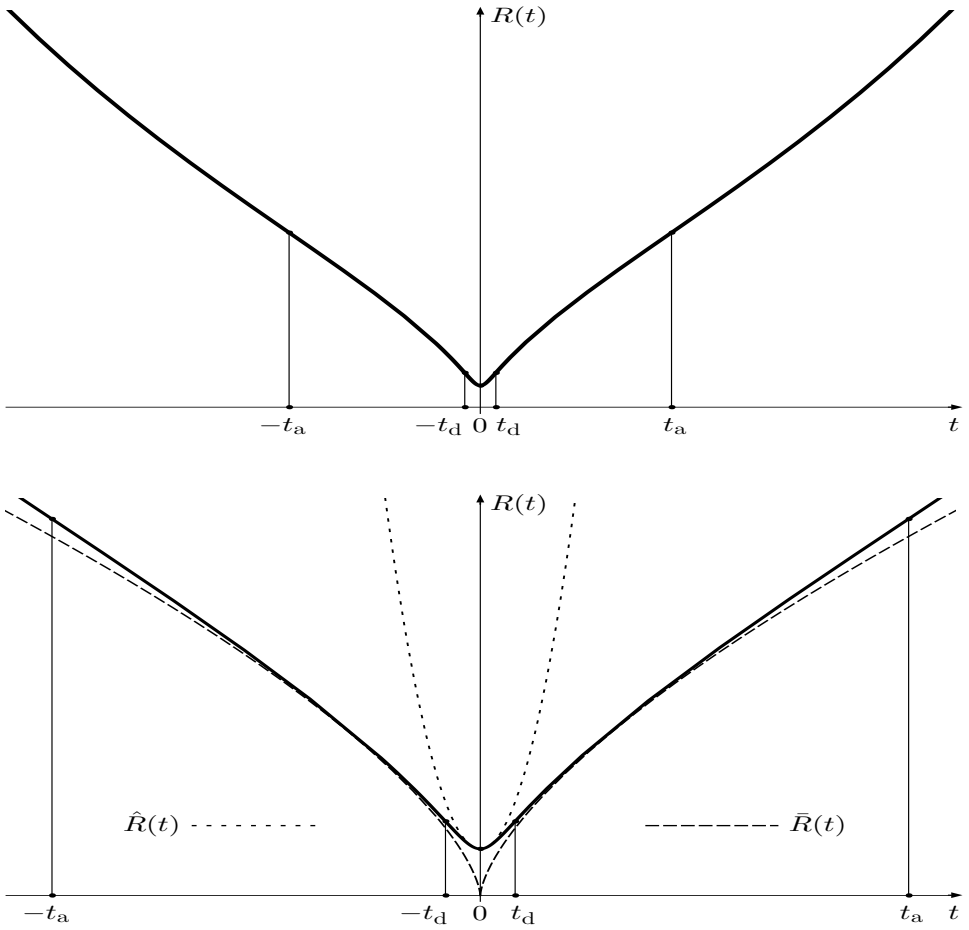

FIG. 4. Graph of $R(t)$ for $k = 0$ and generic positive values of $A_{\rm C}$, $A_{\rm P}$, and B with $B < A_{\rm P}^2/8A_{\rm C}$, showing early acceleration from $t = 0$ to $t = t_{\rm d}$, deceleration from $t_{\rm d}$ to $t_{\rm a}$, and ultimately exponential acceleration after $t_{\rm a}$; truncated graph of $R(t)$ with approximations $\hat{R}(t)$ and $\bar{R}(t)$ as identified in Eqs. (34) and (36).

Equivalent to Eq. (33) is

$$R^3(t) - R_{\rm min}^3 \approx \frac{3A_{\rm C}}{2}\left(R_{\rm min}^3 + \frac{A_{\rm P}}{A_{\rm C}}\right)(c\,t)^2\,. \tag{35}$$

After $R(t)$ has inflated to the point that $R_{\rm min}/R(t) \ll 1$, $(R^3(t) - R_{\rm min}^3)^{\frac{1}{3}}$ will differ but little from $R(t)$, and then, for so long as t remains small enough for the approximate Eq. (33) to hold, the approximation

$$R(t) \approx \bar{R}(t) := \left[\frac{3A_{\rm C}}{2}\left(R_{\rm min}^3 + \frac{A_{\rm P}}{A_{\rm C}}\right)\right]^{\frac{1}{3}}(c\,t)^{2/3} \tag{36}$$

will be valid. The second graph in Fig. 4 shows the approximations $\hat{R}(t)$ and $\bar{R}(t)$.

B. Nonflat open ($k = -1$) and closed ($k = 1$) universes

When $k = -1$ or 1, elementary symbolic solutions of Eqs. (22) and (23) are unavailable, so one must resort to numerical solution of Eq. (23). The integration proceeds most smoothly when carried out for the equivalent equation

$$\ddot{U} = 3c^2A_{\rm C}U - \frac{6c^2k}{R_{\rm min}^2}U^{\frac{1}{3}} + \frac{3c^2A_{\rm P}}{R_{\rm min}^3}\,, \tag{37}$$

where $U \coloneqq S^3$ and $S \coloneqq R/R_{\rm min}$, with initial conditions $U(0) = 1$ and $\dot{U}(0) = 0$, obtained from $S(0) = R(0)/R_{\rm min} = R_{\rm min}/R_{\rm min} = 1$ and $\dot{S}(0) = \dot{R}(0)/R_{\rm min} = 0$. (Note that this equation and the initial conditions apply equally well when $k = 0$.)

To enable the integration, numerical values must be chosen for the parameters other than k that appear in Eq. (37), namely, $A_{\rm C}$, $A_{\rm P}$, and B (implicitly through $R_{\rm min}$). For this determination let us impose the requirement that the solution(s) provide good fits to a Hubble diagram based on data from recent observations of type Ia supernovae. Toward that end a number of definitions are in order:

- t_0, the time of the present epoch, i. e., the time elapsed since the bounce at $t = 0$.
- $H_0 \coloneqq H(t_0)$, the present value of the Hubble parameter.
- $R_0 \coloneqq c/H_0$, usually referred to as the 'Hubble radius' and as the 'radius of the visible universe'.
- $z \coloneqq R(t_0)/R - 1$, the redshift function.
- $z_{\rm d} \coloneqq R(t_0)/R_{\rm d} - 1$ and $z_{\rm a} \coloneqq R(t_0)/R_{\rm a} - 1$, the redshifts associated with the transitions from acceleration to deceleration and from deceleration back to acceleration.
- $\tilde{R} \coloneqq R/R(t_0) = 1/(1+z)$, a conventional notation.
- $\tilde{R}_{\rm min} \coloneqq R_{\rm min}/R(t_0)$ and $\tilde{R}_{\{\rm d,a\}} \coloneqq R_{\{\rm d,a\}}/R(t_0)$.
- $\lambda \coloneqq c/H_0 R(t_0) = R_0/R(t_0)$, a useful parameter.
-

$$\Omega_{\rm C} \coloneqq \frac{c^2}{3H_0^2} A_{\rm C}\,, \tag{38}$$

$$\Omega_{\rm k} \coloneqq -\frac{c^2}{H_0^2 R^2(t_0)} k = -\lambda^2 k\,, \tag{39}$$

$$\Omega_{\rm P} \coloneqq \frac{2c^2}{3H_0^2 R^3(t_0)} A_{\rm P} = \frac{2H_0\lambda^3}{3c} A_{\rm P}\,, \tag{40}$$

and

$$\Omega_{\rm B} \coloneqq -\frac{c^2}{3H_0^2 R^6(t_0)} B = -\frac{H_0^4\lambda^6}{3c^4} B\,. \tag{41}$$

With these definitions Eq. (22) is equivalent to

$$H^2 = H_0^2 \left(\Omega_{\rm C} + \Omega_{\rm k} \frac{1}{\tilde{R}^2} + \Omega_{\rm P} \frac{1}{\tilde{R}^3} + \Omega_{\rm B} \frac{1}{\tilde{R}^6} \right)\,, \tag{42}$$

which upon evaluation at t_0 yields

$$\Omega_{\rm C} + \Omega_{\rm k} + \Omega_{\rm P} + \Omega_{\rm B} = 1\,. \tag{43}$$

On the other hand, Eq. (23) is equivalent to

$$\frac{\ddot{\tilde{R}}}{\tilde{R}} = H_0^2 \left(\Omega_{\rm C} - \frac{1}{2}\,\Omega_{\rm P} \frac{1}{\tilde{R}^3} - 2\,\Omega_{\rm B} \frac{1}{\tilde{R}^6} \right) \tag{44}$$

$$= H_0^2 \frac{2\,\Omega_{\rm C}\tilde{R}^6 - \Omega_{\rm P}\tilde{R}^3 - 4\,\Omega_{\rm B}}{2\,\tilde{R}^6}\,, \tag{45}$$

which yields, as roots of $\ddot{\tilde{R}} = 0$,

$$\tilde{R}_{\rm d} \coloneqq \left(\frac{\Omega_{\rm P}}{4\,\Omega_{\rm C}} - \frac{\sqrt{\Omega_{\rm P}^2 + 32\,\Omega_{\rm C}\,\Omega_{\rm B}}}{4\,\Omega_{\rm C}} \right)^{\frac{1}{3}} \tag{46}$$

and

$$\tilde{R}_{\rm a} \coloneqq \left(\frac{\Omega_{\rm P}}{4\,\Omega_{\rm C}} + \frac{\sqrt{\Omega_{\rm P}^2 + 32\,\Omega_{\rm C}\,\Omega_{\rm B}}}{4\,\Omega_{\rm C}} \right)^{\frac{1}{3}} \tag{47}$$

(obtainable also from Eqs. (26) and (27) by substitution from Eqs. (38), (40), and (41)).

To produce a curve to match against the data points of a Hubble diagram one needs the following standard formula for the luminosity distance $D_{\rm L}$ of a photon-emitting astronomical object at redshift z:

$$D_{\rm L}(z) = (1+z) R(t_0)\, r_{\rm k} \left(\frac{c}{R(t_0)} \int_0^z \frac{1}{\overset{*}{H}(u)}\, du \right) . \tag{48}$$

Here

$$r_{\rm k}(\rho) \coloneqq \begin{cases} \sinh\rho & \text{if} \quad k = -1, \\ \rho & \text{if} \quad k = 0, \\ \sin\rho & \text{if} \quad k = 1, \end{cases} \tag{49}$$

and

$$\overset{*}{H}(z) \coloneqq H_0 [\Omega_{\rm C} + \Omega_{\rm k}(1+z)^2 + \Omega_{\rm P}(1+z)^3 + \Omega_{\rm B}(1+z)^6]^{\frac{1}{2}} . \tag{50}$$

In terms of the parameter λ the luminosity distance formula reads

$$D_{\rm L}(z) = (1+z) \frac{c}{\lambda H_0}\, r_{\rm k} \left(\lambda \int_0^z \frac{du}{[\Omega_{\rm C} + \Omega_{\rm k}(1+u)^2 + \Omega_{\rm P}(1+u)^3 + \Omega_{\rm B}(1+u)^6]^{\frac{1}{2}}} \right) . \tag{51}$$

From D_L one constructs the distance modulus $\boldsymbol{\mu}$, the difference between the apparent magnitude and the absolute magnitude of the object in question at redshift z; this reduces in the usual way to

$$\boldsymbol{\mu}(z) = 5 \log_{10} \left(\frac{D_L(z)}{10\,\text{pc}} \right) = 25 + \log_{10} \left(\frac{D_L(z)}{1\,\text{Mpc}} \right) . \tag{52}$$

From $\tilde{R} = 1/(1+z)$ follows $-\dot{z}/(1+z) = \dot{\tilde{R}}/\tilde{R} = \overset{*}{H}(z)$, thus $dz/dt = -(1+z)\overset{*}{H}(z)$, which upon integration yields the following formula for the time $T(z)$ elapsed between an event occurring at redshift z and the present time t_0 (when $z = 0$):

$$T(z) = \int_0^z \frac{1}{(1+u)\overset{*}{H}(u)}\, du = \frac{1}{H_0} \int_0^z \frac{du}{(1+u)[\Omega_{\rm C} + \Omega_{\rm k}(1+u)^2 + \Omega_{\rm P}(1+u)^3 + \Omega_{\rm B}(1+u)^6]^{\frac{1}{2}}} . \tag{53}$$

The distance modulus $\boldsymbol{\mu}$ of Eq. (52) is the function to be fitted to the relative magnitudes data obtained from observations of type Ia supernovae. The SNe Ia data to be used are those from the 182-member gold sample described in Sec. 3 of [14], provided at `http://braeburn.pha.jhu.edu/~ariess/R06/sn_sample`, the ith data point consisting of an observed relative magnitude $\boldsymbol{\mu}_i$ of a supernova, the redshift z_i of that supernova, and the standard deviation σ_i of the observations used in the determination of $\boldsymbol{\mu}_i$. The requisite calculations are carried out (using the indicated Mathematica functions) in two stages, the first of which comprises the following steps:

1. On first run, set $H_0 = 73.8$ km s^{-1}/Mpc, the recent estimate of H_0 obtained by Riess, et al. [15]. On subsequent runs set $H_0 = 71.4$ km s^{-1}/Mpc and $H_0 = 76.2$ km s^{-1}/Mpc, the extremes of the 3.3% confidence interval predicted in [15].

2. Set $B = 0$, thus $\Omega_{\rm B} = 0$. This makes $R_{\rm d} = R_{\rm min} = 0$, so will produce a 'big bang' model with $z_{\rm d} = \infty$ and with no inflation (cf. Eq. (23), in which the last term, now absent, is the one that makes $\ddot{R}$ large when $R \approx 0$).

3. For $k = 0$, using NIntegrate as the integrator for $D_{\rm L}(z)$ in Eq. (51), apply NonlinearModelFit to $\boldsymbol{\mu}(z)$ to obtain, subject to the constraint of Eq. (43), Chi-square best-fit values for $\Omega_{\rm P}$, $\Omega_{\rm C}$, and λ. Do the same for $k = -1$ and $k = 1$. (Note that when $k = 0$, λ disappears from Eq. (51), so is irrelevant to the fitting.)

4. From the best-fit values thus obtained, compute $\tilde{R}_{\rm a}$ from Eq. (47), then $z_{\rm a}$ from $\tilde{R}_{\rm a} = 1/(1+z_{\rm a})$.

5. From Eq. (53), by applying NDSolve to the initial-value problem $dT/dz = 1/(1+z)\overset{*}{H}(z)$, $T(0) = 0$, compute $T(z)$ and then the implied time elapsed since the big bang as $\lim_{z\to\infty} T(z)$.

6. Compute the reduced Chi-square statistic for 180 degrees of freedom (182 for the data, minus 2 for the three parameters $\Omega_{\rm P}$, $\Omega_{\rm C}$, and λ with the one dependency $\Omega_{\rm C} = 1 - \Omega_{\rm P} + \lambda^2 k$):

$$\chi^2_{\rm red} \coloneqq \frac{\chi^2}{180} \quad \text{and} \quad \chi^2 \coloneqq \sum_{i=1}^{182} \left(\frac{\boldsymbol{\mu}(z_i) - \boldsymbol{\mu}_i}{\sigma_i} \right)^2 . \tag{54}$$

Table I presents the results of these computations.

To prepare for the second stage observe that Eqs. (46) and (47) imply that

$$\Omega_{\rm P} = 2\,(\tilde{R}_{\rm d}^3 + \tilde{R}_{\rm a}^3)\,\Omega_{\rm C} \quad \text{and} \quad \Omega_{\rm B} = -\tfrac{1}{2}\,\tilde{R}_{\rm d}^3\,\tilde{R}_{\rm a}^3\,\Omega_{\rm C}\,. \tag{55}$$

Equivalent to Eq. (43) is $\Omega_{\rm C} + \Omega_{\rm P} + \Omega_{\rm B} = 1 - \Omega_{\rm k}$, substitution into which from Eqs. (55), then back into Eqs. (55), yields

$$\Omega_{\rm C} = \frac{1 - \Omega_{\rm k}}{1 + 2\,(\tilde{R}_{\rm d}^3 + \tilde{R}_{\rm a}^3) - \frac{1}{2}\,\tilde{R}_{\rm d}^3\,\tilde{R}_{\rm a}^3}\,, \tag{56}$$

$$\Omega_{\rm P} = \frac{2\,(\tilde{R}_{\rm d}^3 + \tilde{R}_{\rm a}^3)(1 - \Omega_{\rm k})}{1 + 2\,(\tilde{R}_{\rm d}^3 + \tilde{R}_{\rm a}^3) - \frac{1}{2}\,\tilde{R}_{\rm d}^3\,\tilde{R}_{\rm a}^3}\,, \tag{57}$$

and

$$\Omega_{\rm B} = \frac{-\frac{1}{2}\,\tilde{R}_{\rm d}^3\,\tilde{R}_{\rm a}^3\,(1 - \Omega_{\rm k})}{1 + 2\,(\tilde{R}_{\rm d}^3 + \tilde{R}_{\rm a}^3) - \frac{1}{2}\,\tilde{R}_{\rm d}^3\,\tilde{R}_{\rm a}^3}\,, \tag{58}$$

where, from Eq. (39), $\Omega_{\rm k} = -\lambda^2 k$.

Because the supernovae data extend into the past only to $z = 1.755$ (SN 1997ff), the best-fit parameters $\Omega_{\rm P}$, $\Omega_{\rm C}$, and λ will change by negligible amounts when $\Omega_{\rm B}$ changes from 0 to a small nonzero number. For this reason a different strategy is called for in the second stage, as detailed in the following steps:

7. Set λ and $z_{\rm a}$ to the best-fit values found in the first stage (for $k = 0$, set λ to any positive number). Assign $z_{\rm d}$ a large value.

TABLE I. Best-fit parameters (λ not shown) for 'big bang' model: B set to 0, thus $\Omega_{\rm B} = 0$, so $R_{\rm d} = R_{\rm min} = 0$ and $z_{\rm d} = \infty$.

Inputs		Outputs						
H_0 (km s^{-1}/Mpc)	k	$\Omega_{\rm P}$	$\Omega_{\rm C}$	$\Omega_{\rm k}$	$\tilde{R}_{\rm a}$	$z_{\rm a}$	$\lim_{z\to\infty} T(z)$ (Gyr)	$\chi^2_{\rm red}$
71.4	-1	0.389	0.611	3.07×10^{-12}	0.693	0.465	12.27	0.891
	0	0.389	0.611	0	0.683	0.465	12.27	0.891
	1	0.441	0.690	-0.131	0.684	0.462	12.22	0.890
73.8	-1	0.307	0.693	9.80×10^{-12}	0.605	0.652	12.69	0.888
	0	0.307	0.693	0	0.605	0.652	12.69	0.888
	1	0.479	0.954	-0.433	0.631	0.585	12.52	0.869
76.2	-1	0.239	0.762	6.66×10^{-15}	0.539	0.856	13.19	0.946
	0	0.239	0.762	0	0.539	0.856	13.19	0.946
	1	0.495	1.158	-0.653	0.598	0.673	12.88	0.889

8. From $\tilde{R} = 1/(1+z)$, compute $\tilde{R}_{\rm d}$ and $\tilde{R}_{\rm a}$ (reversing, in the latter case, the computation of $z_{\rm a}$ from $\tilde{R}_{\rm a}$ in the first stage).

9. Using Eqs. (56), (57), (58), and $\Omega_{\rm k} = -\lambda^2 k$, compute $\Omega_{\rm C}$, $\Omega_{\rm k}$, $\Omega_{\rm P}$, and $\Omega_{\rm B}$, and in turn $D_L(z)$ and $\boldsymbol{\mu}(z)$ from Eqs. (51) and (52), applying NDSolve to the initial-value problem $dI/dz = H_0/\overset{*}{H}(z)$, $I(0) = 0$ to compute the integral in Eq. (51).

10. Compute the reduced Chi-square statistic and compare it to the corresponding number from the first stage. If it is appreciably larger, make $z_{\rm d}$ larger, thus $R_{\rm d}$ smaller and $\Omega_{\rm B}$ closer to 0.

11. When a good match is found in Step 10, recover $A_{\rm C}$, $A_{\rm P}$, and B from Eqs. (38), (40), and (41), then $R_{\rm min}$ from $P_1(R_{\rm min}) = 0$ (cf. Eq. (24)) using NSolve.

With $A_{\rm C}$, $A_{\rm P}$, B, and $R_{\rm min}$ in hand, proceed to the solution by NDSolve of Eq. (37) for $U(t)$ and $S(t) = [U(t)]^{\frac{1}{3}}$, with $U(0) = 1$ and $\dot{U}(0) = 0$, to obtain a full history of the model universe. As a check use FindRoot to get t_0 from $\dot{S}(t_0)/S(t_0) = H(t_0) = H_0$ and compare it to $T(z_{\rm min})$ from Eq. (53) (see Step 5), where $1 + z_{\rm min} = R(t_0)/R_{\rm min} = S(t_0) = R_0/\lambda R_{\rm min}$. They must agree.

One can find t_{100}, the time at which R has doubled in size one hundred times from its minimum size at the bounce, by solving the equation $\log_2 S(t) = 100$ using FindRoot. If a different value for t_{100} is wanted, change $z_{\rm d}$ and repeat Steps 7–11 and the integration of Eq. (37). Table II presents results of the second-stage computations.

Figure 5 shows the best-fit models of $\boldsymbol{\mu}(z)$ for $k = 1$, plotted against the 182 SNe Ia gold sample data points they are fitted to. The parameters are those of Table II. The corresponding plots for $k = -1$ and $k = 0$ are visually indistinguishable from the ones shown.

Figure 6 exhibits a complete postbounce history of the best-fit model for $H_0 = 73.8$ km s^{-1}/Mpc and $k = 1$. The parameter values that enter into the numerical solution of Eq. (37) are $A_{\rm C} = 1.821\times10^{-56}$ cm^{-2}, $A_{\rm P} = 3.161\times10^{28}$ cm, and $B = 1.092\times10^{-82}$ cm^4, obtained from the best-fit parameters $\Omega_{\rm C}$, $\Omega_{\rm P}$, and $\Omega_{\rm B}$ by use of Eqs. (38), (40), and (41). The history comprises a brief interval of rapid inflation from the bounce, sliding into deceleration and a graceful exit into an era of coasting, followed by a return to ultimately exponential acceleration at $z = z_{\rm a} = 0.585$ (when $t = 7.06$ Gyr). In the coasting era $Q(t) \approx Q_{\rm min} \gtrsim -0.5$, reflective of the approximate proportionality $R(t) \propto (ct)^{2/3}$ implied by Eq. (36). At $t = t_0$, $Q(t) = 1.292$. Because $k = 1$, $R_{\rm min}$ ($= 2.200\times10^{-37}$ cm) and $R(t_0)$ ($= 1.905\times10^{28}$ cm $= 2.014\times10^{10}$ ly $= 6.174\times10^{3}$ Mpc) are the geometric radii of the model spherical universe at the time of the bounce and at the present time, but these radii are highly dependent on the rather arbitrary setting of $z_{\rm d}$, chosen here to make $t_{100} \approx 10^{-35}$ seconds. Numerical integration of Eq. (37) for $k = -1$ and for $k = 0$, with H_0 the same, yields graphs visually indistinguishable from that in the figure.

TABLE II. Best-fit parameters for 'bounce' model: $B > 0$, thus $\Omega_{\rm B} < 0$ and $R_{\rm min} > 0$. (The columns for $\Omega_{\rm P}$, $\Omega_{\rm C}$, and $\Omega_{\rm k}$ are identical to those of Table I, and are included by reference.)

Inputs					Outputs			
H_0 (km s^{-1}/Mpc)	k	λ	$z_{\rm a}$	$z_{\rm d}$	$\Omega_{\rm B}$	t_{100} (s)	t_0 (Gyr)	$\chi^2_{\rm red}$
71.4	-1	1.75×10^{-6}	0.465	1×10^{65}	-9.72×10^{-197}	1.04×10^{-35}	12.27	0.891
	0	any positive number	0.465	1×10^{97}	-9.72×10^{-293}	5.49×10^{-35}	12.27	0.891
	1	0.363	0.462	1×10^{65}	-1.10×10^{-196}	9.79×10^{-36}	12.22	0.890
73.8	-1	3.13×10^{-6}	0.652	1×10^{65}	-7.69×10^{-197}	1.13×10^{-35}	12.69	0.888
	0	any positive number	0.652	1×10^{97}	-7.69×10^{-293}	6.33×10^{-36}	12.69	0.888
	1	0.658	0.585	1×10^{65}	-1.20×10^{-196}	9.09×10^{-36}	12.52	0.869
76.2	-1	8.16×10^{-8}	0.856	1×10^{65}	-5.96×10^{-197}	1.25×10^{-35}	13.19	0.946
	0	any positive number	0.856	1×10^{97}	-5.96×10^{-293}	6.04×10^{-36}	13.19	0.946
	1	0.808	0.673	1×10^{65}	-1.24×10^{-196}	8.66×10^{-36}	12.88	0.889

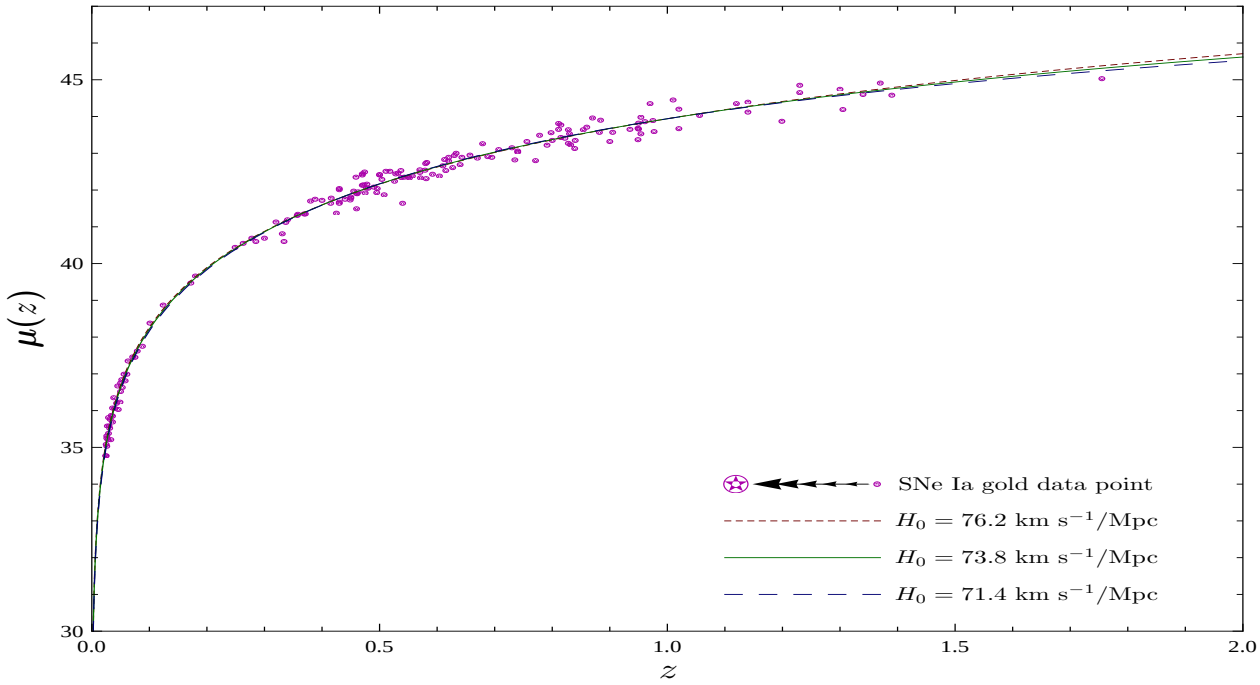

FIG. 5. Best-fit models of $\boldsymbol{\mu}(z)$ for $k = 1$ (parameters shown in Tables II and I), plotted against the 182 SNe Ia gold sample data points they are fitted to. The curve for $H_0 = 73.8$ km s^{-1}/Mpc fits the 182 data points with $\chi^2_{\rm red} = 0.869$.

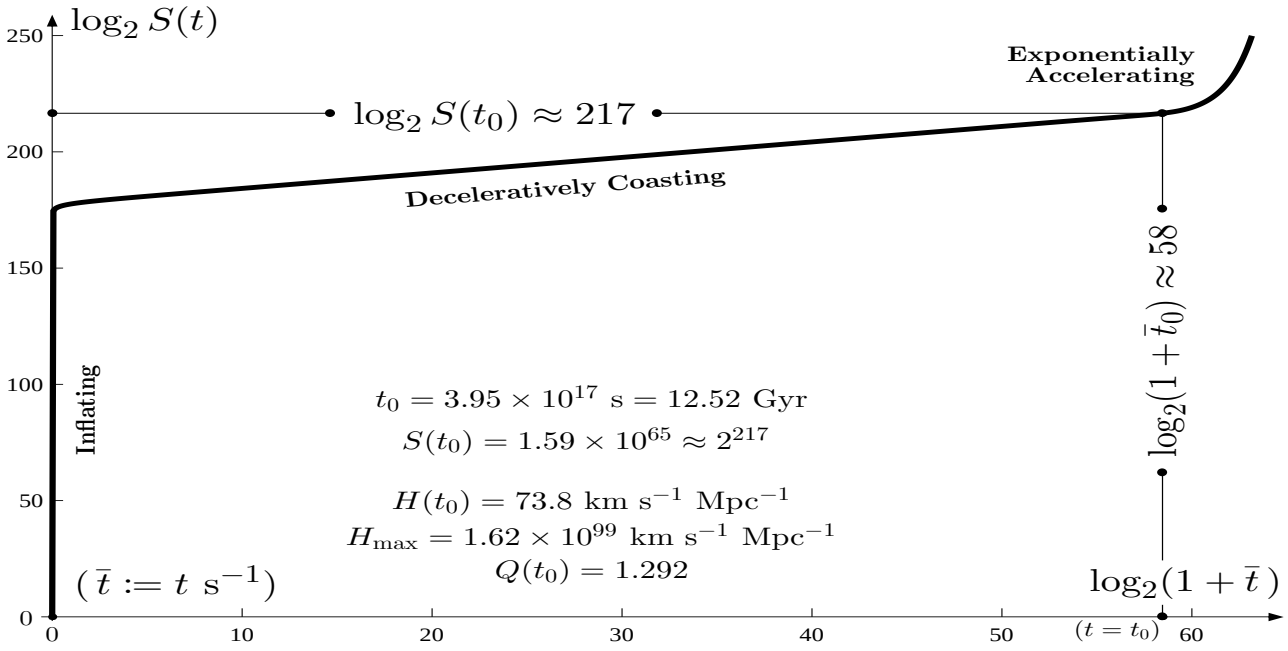

FIG. 6. Postbounce graph of $\log_2 S(t)$ versus $\log_2(1+\bar{t}\,)$ ($\bar{t} := t$ s^{-1}) for the best-fit solution with $H_0 = 73.8$ km s^{-1}/Mpc and $k = 1$. The early stage rapid inflation, after producing 178 doublings of the normalized scale factor S ($:= R/R_{\rm min}$) in the first second after the bounce, gives way smoothly to a period of uphill, decelerative 'coasting' (where the graph is nearly linear). Initially, the acceleration parameter $Q := (\ddot{R}/R)/(\dot{R}/R)^2 = (\ddot{S}/S)/(\dot{S}/S)^2$ is positive and huge ($Q(0) = \infty$). In the coasting period $Q(t) \approx Q_{\rm min} \gtrsim -0.5$, which is reflected in the observation that in that interval $\log_2 S(t) \approx 178 + \frac{217-178}{58-0}\log_2(1+\bar{t}\,) \approx 178 + \frac{2}{3}\log_2(1+\bar{t}\,)$, so that $S(t) \approx 2^{178}(1+\bar{t}\,)^{\frac{2}{3}} \approx 2^{178}\bar{t}^{\,\frac{2}{3}}$ ($S(t) \propto \bar{t}^{\,\frac{2}{3}} \implies Q(t) \equiv -\frac{1}{2}$). After the coasting era $Q(t)$ becomes positive again at redshift $z_{\rm a} = 0.585$ (when $t = 7.06$ Gyr and $\log_2(1+\bar{t}\,) = 57.6$), rising to 1.292 at $t = t_0$, and then to a maximum of 1.310 at $t = 14.24$ Gyr before settling asymptotically to 1 as $t \to \infty$, the growth rate of $S(t)$ thus asymptotically becoming exponential as in a de Sitter universe. The corresponding graphs for the best-fit solutions with H_0 the same and $k = -1$ and $k = 0$ are not appreciably different from this one.

VI. DARK MATTER AND DARK 'ENERGY'

A. Drainholes

The 'drainhole' model of a gravitating particle developed in [1] and proposed as a source for the negative, gravitationally repulsive mass density $\bar{\mu}$ in the action integral of Eq. (6) is a static, spherically symmetric, vacuum ($\mu = \bar{\mu} = 0$) solution of the same field equations (7) that the cosmological model of the preceding sections is a solution of, but with $\psi = 0$.[2,3] This space-time manifold has come to be recognized as an early (apparently the earliest) example of what is now called by some a 'traversable wormhole' [16], and has been analyzed from various perspectives by others [17–29]. Its metric has the proper-time forms

$$c^2 d\tau^2 = [1 - f^2(\rho)]\, c^2 dT^2 - \frac{1}{1 - f^2(\rho)}\, d\rho^2 - r^2(\rho)\, d\Omega^2 \tag{59}$$

$$= c^2 dt^2 - [d\rho - f(\rho)\, c\, dt]^2 - r^2(\rho)\, d\Omega^2\,, \tag{60}$$

where $t = T - \dfrac{1}{c}\displaystyle\int \frac{f(\rho)}{1 - f^2(\rho)}\, d\rho$,

$$f^2(\rho) = 1 - e^{-(2\,m/n)\alpha(\rho)}\,, \tag{61}$$

$$r(\rho) = \sqrt{(\rho - m)^2 + a^2}\, e^{(m/n)\alpha(\rho)}\,, \tag{62}$$

and

$$\phi = \alpha(\rho) = \frac{n}{a}\left[\frac{\pi}{2} - \tan^{-1}\left(\frac{\rho - m}{a}\right)\right]\,, \tag{63}$$

with $a := \sqrt{n^2 - m^2}$, the parameters m and n satisfying $0 \leq m < n$. (The coordinate ρ used here translates to $\rho + m$ in [1].) The shapes and linear asymptotes of r and f^2 are shown in Fig. 7. Not obvious, but verifiable, is that $f^2(\rho) \sim 2\,m/\rho$ as $\rho \to \infty$, which, together with $r(\rho) \sim \rho$ as $\rho \to \infty$, shows m to correspond to the Schwarzschild mass parameter.

The shared metric of the cross sections of constant t is $d\rho^2 + r^2(\rho)\, d\Omega^2$. The choke surface of the drainhole throat (where $r(\rho)$ is a minimum) is the 2-sphere at $\rho = 2\,m$, of areal radius $r(2\,m) = ne^{(m/n)\alpha(2\,m)}$, which increases monotonically from n to ne as m increases from 0 to n. Thus the size of the throat is determined primarily by n, and only secondarily by m. Moreover, as indicated by the calculation that the contracted curvature tensor $\mathbf{Ricci} = -2(d\phi \otimes d\phi) = (-n^2/[(\rho - m)^2 + a^2]^2)(d\rho \otimes d\rho)$, the strength of ϕ's 'contribution' to the space-time geometry is determined primarily by n and is concentrated on the curvature of space, providing the negative spatial curvatures necessary for the open throat to exist. In accord with the restriction adopted here that the 'relaxant' scalar fields ϕ and ψ in the action integral of Eq. (6) were not to be varied in deriving the field equations, one would not say that ϕ *causes* (i. e., is a source of) these spatial curvatures, but should instead say that ϕ allows and tells of the existence of such negative curvatures and describes their configuration. This understanding helps disabuse one of the notion that geometrically and topologically unexceptionable space-time manifolds such as the drainhole are somehow a product of 'exotic' matter just because their Ricci tensors disrespect some 'energy condition' that traces back to Einstein's unjustified 1916 assumption.

Even when $m = 0$, so that there is no gravity, the throat stays open, with $r(\rho) = \sqrt{\rho^2 + n^2}$. It is not a great stretch to surmise that, whereas the parameter m specifies the active gravitational mass of the (nonexotic) drainhole particle, the parameter n specifies in some way its inertial rest mass. This speculation is supported by two considerations: first, as shown in [1], the total 'energy' of the scalar field ϕ lies in the interval from $n/2$ to $n\pi/2$, thus is essentially proportional to n; second, it would seem likely that the bigger the hole (thus the larger is n), the greater the force needed to make it move. A 'higgsian' way of expressing this idea is to say that the drainhole 'acquires' (inertial) mass from the scalar field ϕ.

Because $r(\rho) \geq n > 0$ and $f^2(\rho) < 1$, the drainhole space-time manifold is geodesically complete and has no one-way event horizon, the throat being therefore traversable by test particles and light in both directions. The vector field

---

[2] $\boldsymbol{R}_{\alpha\beta}$ and $\boldsymbol{R}$ here are the negatives of those in [1].

[3] The scalar field ϕ was presumed in [1] to satisfy the wave equation $\Box\phi = 0$ obtained from allowing ϕ to vary in the action integral. In retrospect, however, that is seen to have been a redundancy, as the field equations (8), which follow from variation of the metric alone, reduce when $\psi = 0$ to $2\,(\Box\phi)\phi_{.\alpha} = 0$, a consequence of which is $\Box\phi = 0$.

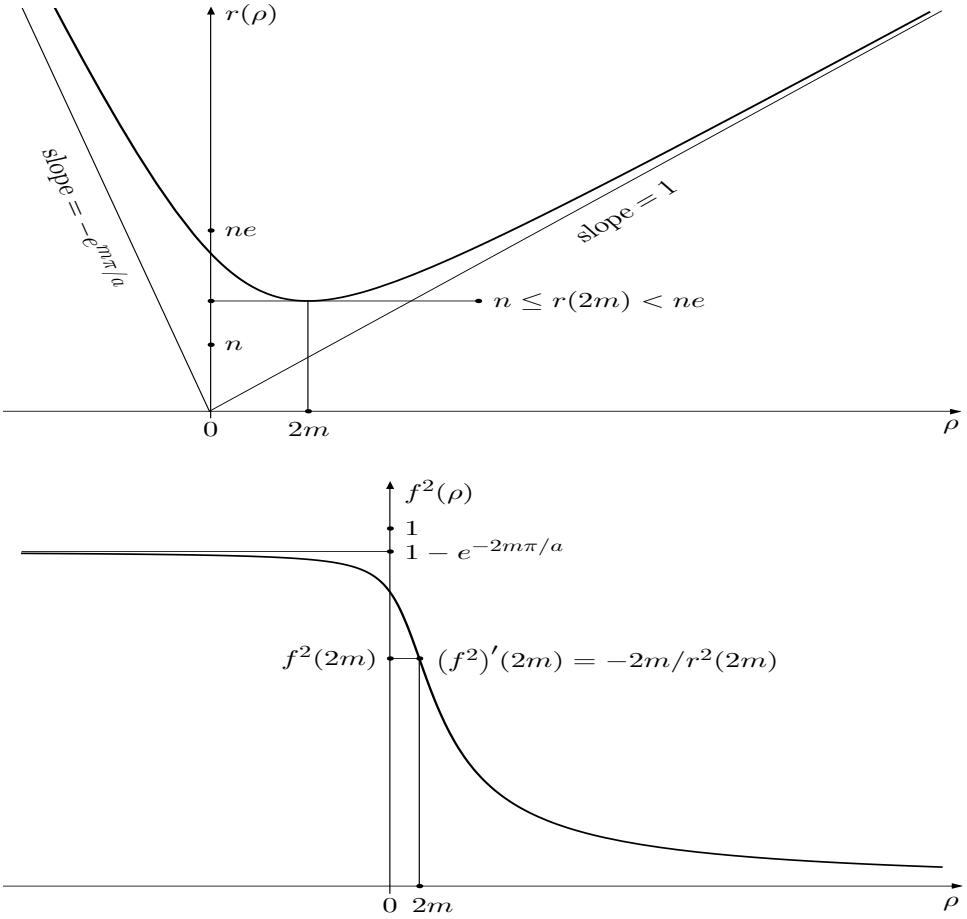

FIG. 7. Graphs of $r(\rho)$ and $f^2(\rho)$ for generic values of the parameters m and n ($0 \le m < n$ and $a \coloneqq \sqrt{n^2 - m^2}$).

$\partial_t + cf(\rho)\partial_\rho$ generates radial geodesics parametrized by proper time; with f chosen as $-\sqrt{f^2}$ it is taken to be the velocity field of a 'gravitational ether' flowing from the high side (where $\rho > 2m$) down through the drainhole and out into the low side (where $\rho < 2m$). The ether's radial acceleration is $(c^2 f^2/2)'(\rho)$, which computes to $-c^2 m/r^2(\rho)$ and therefore is strongest at $\rho = 2\,m$, where r assumes its minimum value. Because the radial acceleration is everywhere aimed in the direction of decreasing ρ, the drainhole attracts test particles on the high side and repels them on the low side. Moreover, as demonstrated in [1] by means of an isometry of the manifold that exchanges the upper and lower regions with one another, whereas the upper region is asymptotic as $\rho \to \infty$ to a Schwarzschild manifold with (active gravitational) mass parameter m, the lower region is asymptotic as $\rho \to -\infty$ to a Schwarzschild manifold with mass parameter $\bar{m} = -me^{m\pi/a}$, so the drainhole repels test particles more strongly on the low side than it attracts them on the high side, in the ratio $-\bar{m}/m = e^{m\pi/\sqrt{n^2-m^2}}$. It is this excess of negative, repulsive mass over positive, attractive mass that qualifies drainholes as candidates for explaining the accelerating expansion of the universe and doing away with the cosmological constant.

As mentioned in the Introduction, one can imagine that, instead of a not well defined 'gravitational ether', it is space itself that flows into and through the drainhole.[4] This substitution, which as noted in the Introduction is in accord with Einstein's insight that the concepts of space and of a gravitational ether are essentially interchangeable, should cause no alarm, for the very notion of an expanding universe already ascribes to space the requisite plasticity.

The discovery of the drainhole manifolds arose, in my case, from a search for a model for gravitating particles that, unlike a Schwarzschild space-time manifold, would have no singularity. Geodesic completeness and absence of event horizons resulted naturally from that requirement and the utilization of a minimally coupled scalar field to weaken the field equations. As shown in [1], a drainhole possesses all the geodesic properties that a Schwarzschild blackhole possesses other than those that depend on the existence of its horizon and its singularity, having eliminated

[4] This idea has been applied in [30] to the interpretation and visualization of blackholes, with interesting results.

the horizon and replaced the singularity with a topological passageway to another region of space. Drainholes are able, therefore, to reproduce all the externally discernible aspects of physical blackholes (if such things exist) that Schwarzschild blackholes reproduce. That their low sides have never been knowingly observed (but in principle could be) is no more troubling than the impossibility of directly observing the insides of Schwarzschild blackhole horizons from external vantage points. For these reasons drainholes are more satisfactory than Schwarzschild blackholes as mathematical models of centers of gravitational attraction. Moreover, there is little reason to doubt that rotating drainhole manifolds analogous to the Kerr rotating blackhole manifolds exist and will prove to be better models than the Kerr manifolds. (A relatively recent solution of the field equations (7) and (8) perhaps describes such a manifold [28]).

B. Dark matter and dark 'energy' from drainholes

A physical center of attractive gravity modeled by a drainhole could justifiably be called a 'darkhole', inasmuch as (as shown in [1]) it would capture photons (and other particles) that venture too close, but, unlike a blackhole, must eventually release them, either back to the attracting high side whence they came or down through the drainhole and out into the repelling low side. Thus one can imagine that at active galactic centers will be found not supermassive blackholes, but supermassive darkholes. At the center of our galaxy, for example, instead of a blackhole of Schwarzschild mass $m \approx 4 \times 10^6 M_\odot \approx 1.18 \times 10^7$ km (in geometric units), and of horizon area $4\pi(2\,m)^2 \approx 4.39 \times 10^{14}$ km^2, there might reside a drainhole the area $4\pi r^2(2\,m)$ of whose choke sphere would lie between $4\pi n^2$ and $4\pi(ne)^2$, with n constrained only by having to exceed m. As measured by the bounds n and ne on the areal radius $r(2\,m)$, and the corresponding bounds $m/n^2 = (m/n)(1/n)$ and $m/(ne)^2 = (m/n)(1/e^2 n)$ on the maximum radial acceleration $m/r^2(2\,m)$, with m constrained by $0 \leq m < n$, such an object could be of any size and could be weakly gravitating for its size ($m \ll n$), strongly gravitating for its size ($m \approx n$), or anything in between.

There is, however, more to be said. A central tenet of the general theory of relativity is that every object that gravitates, no matter how large or how small, is a manifestation of a departure of the geometry of space-time from flatness. If such an object has other, nongravitational properties, these must be either incorporated in or additional to the underlying geometric structure. Believing that the drainhole model provides the best presently available description of a gravitating particle's geometry, I therefore adopt the hypothesis that every such *elementary* gravitating object is at its core an actual physical drainhole — these objects to include not only elementary constituents of visible matter such as protons and neutrons (or perhaps, more elementarily, quarks), but also the unseen particles of 'dark matter' whose existence is at present only inferential. Moreover, I will consider that visible matter and the primordial matter of my cosmological model are, gravitationally, one and the same, and that the continuously created matter of the model is composed of particles that are drainholes with no additional properties.

The pure, isolated drainhole described by Eqs. (59–63) is an 'Einstein–Rosen bridge' connecting two otherwise disjoint 'subuniverses' [31], each of which, if evolving, would by itself consume for its description all the resources of a Robertson–Walker metric. Nonisolated drainholes presumably could exist not only as 'bridges' between our subuniverse and another (or multiple others), but also as 'tunnels' from one place in our subuniverse to another, possibly quite distant from the first by every route that doesn't take a shortcut through a tunnel. Both types could contribute to the positive and the negative mass densities μ and $\bar{\mu}$ in our subuniverse, each bridge drainhole contributing to μ or to $\bar{\mu}$, but not to both, each tunnel drainhole contributing both to μ by way of its gravitationally attractive entrance portal and to $\bar{\mu}$ by way of its gravitationally repulsive exit portal. Tunnel drainholes are easy enough to visualize in abundance as topological holes into which flowing space disappears, only to reappear elsewhere in our subuniverse, in analogy with rivers that go underground and surface somewhere downstream. Having both portals located in our subuniverse, tunnel drainholes would have properties we could fully take account of. Bridge drainholes, on the other hand, with only one side in our subuniverse would have properties dependent in part on circumstances in other subuniverses, circumstances beyond our ken. I shall, therefore, assume that no bridge drainholes contribute to μ or to $\bar{\mu}$, that the only contributors are tunnel drainholes, consequently that our subuniverse, even if part of a 'multiverse', is self-contained.

Lacking for the present a full mathematical description of these tunnel drainholes, let us nevertheless proceed under the assumption that they exist and are characterized by parameters m and n related as in an isolated bridge drainhole. Every particle of gravitating matter, whether in the 'primordial' (P) category or the 'continuously created' (C) category, is then at its core one of these tunnels, and it becomes a question of relating m and n to the present-epoch densities $\mu_{\mathrm{P},0}$, $\bar{\mu}_{\mathrm{P},0}$, $\mu_{\mathrm{C},0}$, and $\bar{\mu}_{\mathrm{C},0}$.

The fitting of the cosmological solutions of Sec. V to the SNe Ia data determines, by way of Eqs. (19), (20), (38), and (40), and Table II, the net densities $\mu_{\mathrm{P},0} + \bar{\mu}_{\mathrm{P},0}$ and $\mu_{\mathrm{C},0} + \bar{\mu}_{\mathrm{C},0}$, but tells nothing about the mix between the positive densities and the negative. To 'fix the mix', even if somewhat arbitrarily and only for P-densities, a procedure comes to mind that is based on a comparison between the model in question and the 'standard', or 'concordance',

model. Equation (42) can be recast in the form

$$H^2 = \frac{c^2}{3}A_{\rm C} - \frac{8\pi\kappa}{3}(\mu_{\rm P,0} + \bar{\mu}_{\rm P,0})\frac{1}{\tilde{R}^3} + H_0^2\left(\Omega_{\rm k}\frac{1}{\tilde{R}^2} + \Omega_{\rm B}\frac{1}{\tilde{R}^6}\right) . \tag{64}$$

The analogous equation for the 'concordance' (ΛCDM) model is

$$H^2 = \frac{c^2}{3}\Lambda + \frac{8\pi\kappa}{3}\mu_{\rm M}\frac{1}{\tilde{R}^3} + H_0^2\left(\Omega_{\rm k}\frac{1}{\tilde{R}^2} + \Omega_{\rm R}\frac{1}{\tilde{R}^4}\right) , \tag{65}$$

where the subscripts M and R refer to matter and radiation, respectively. As the only kind of gravitating matter contemplated by the concordance model is effectively primordial matter (existent from the epoch of baryon genesis or earlier, treated in Eq. (65) as if existent from the big bang onward), the density $\mu_{\rm M}$ can be identified with the density $\mu_{\rm P,0}$, and then the corresponding primordial matter terms in the two equations will match exactly if $-(\mu_{\rm P,0} + \bar{\mu}_{\rm P,0}) = \mu_{\rm M} = \mu_{\rm P,0}$, thus if $\bar{\mu}_{\rm P,0}/\mu_{\rm P,0} = -2$.

To produce P-densities in the ratio $\bar{\mu}_{\rm P}/\mu_{\rm P}$ with tunnel particles of uniform masses $m_{\rm P}$ and sizes $n_{\rm P}$ requires that $\bar{\mu}_{\rm P}/\mu_{\rm P} = \bar{m}_{\rm P}/m_{\rm P} = -e^{m_{\rm P}\pi/\sqrt{n_{\rm P}^2 - m_{\rm P}^2}}$, which entails that $\bar{\mu}_{\rm P}/\mu_{\rm P}$ is constant and

$$\left(\frac{m_{\rm P}}{n_{\rm P}}\right)^2 = \frac{[\ln(-\bar{\mu}_{\rm P}/\mu_{\rm P})]^2}{[\ln(-\bar{\mu}_{\rm P}/\mu_{\rm P})]^2 + \pi^2} . \tag{66}$$

If we take $\bar{\mu}_{\rm P,0}/\mu_{\rm P,0} = -2$, then $\bar{\mu}_{\rm P}/\mu_{\rm P} = -2$, and $m_{\rm P}/n_{\rm P} = \ln 2/\sqrt{(\ln 2)^2 + \pi^2} \approx 0.22$. Under the assumption that $n_{\rm P}$, or better, the choke radius $r(2\,m_{\rm P})$, is a proportional measure of the inertial mass of the primordial particles, this fixing of $m_{\rm P}/n_{\rm P}$ would provide a basis outside the context of newtonian physics for suspecting the existence of a uniform ratio of active gravitational mass to passive-inertial mass of those particles. If we adopt this assumption and, as I propose, take the primordial particles to be the gravitational cores of the protons and neutrons of the present epoch, then perhaps $r(2\,m_{\rm P}) = m_{\rm p\text{-}n}$, the inertial mass of a proton or a neutron. Converted to geometric units $m_{\rm p\text{-}n} = 1.67 \times 10^{-24}$ g $= 1.24 \times 10^{-52}$ cm, so that $n_{\rm P} = r(2\,m_{\rm P})e^{-(m_{\rm P}/n_{\rm P})\alpha(2\,m_{\rm P})} = 0.74 m_{\rm p\text{-}n} = 1.24 \times 10^{-24}$ g $= 9.20 \times 10^{-53}$ cm and $m_{\rm P} = 2.67 \times 10^{-25}$ g $= 1.98 \times 10^{-53}$ cm. From Eqs. (19) and (40) one calculates that

$$\mu_{\rm P,0} + \bar{\mu}_{\rm P,0} = -\frac{3H_0^2}{8\pi\kappa}\,\Omega_{\rm P} , \tag{67}$$

which for $H_0 = 73.8$ km s^{-1}/Mpc and the best-fit value $\Omega_{\rm P} = 0.479$ of Table II (cf. Table I) reduces to $\mu_{\rm P,0} + \bar{\mu}_{\rm P,0} = -4.90 \times 10^{-30}$ g/cm^3 $= -3.64 \times 10^{-58}$ cm/cm^3. With $\bar{\mu}_{\rm P,0}/\mu_{\rm P,0} = -2$ this gives $\mu_{\rm P,0}/m_{\rm P} = 18.3/{\rm m}^3$ as the present proton-neutron (*qua* primordial particle) number density.

Comparison of the terms $c^2A_{\rm C}/3$ and $c^2\Lambda/3$ in Eqs. (64) and (65) serves only to provide an identity for Λ, so to 'fix the mix' of positive and negative densities in $\mu_{\rm C,0} + \bar{\mu}_{\rm C,0}$ requires a strategy different from that used for $\mu_{\rm P,0} + \bar{\mu}_{\rm P,0}$. Note that, unlike the concordance model, which combines the gravitational effects of baryonic (visible) matter and cold dark matter in the term $(8\pi\kappa/3)(\mu_{\rm M}/\tilde{R}^3)$ in Eq. (65) and thereby predicts from observational data a cold dark matter (CDM) to baryonic matter (BM) mass ratio of approximately 4:1, presumably constant in time, the model developed here reserves the analogous term in Eq. (64) for the effects of baryonic matter alone. That leaves the CDM to BM ratio, specified here as $\mu_{\rm C}/\mu_{\rm P}$, undetermined, and moreover allows it to be time-dependent, inasmuch as $\mu_{\rm C} + \bar{\mu}_{\rm C}$ is constant and $\mu_{\rm P} + \bar{\mu}_{\rm P} \propto R^{-3}$. To generate estimates for C-matter like those for P-matter, let us set $\gamma(z) \coloneqq \mu_{\rm C}(t)/\mu_{\rm P}(t)$, where t is the epoch of events seen at redshift z, and use $\gamma_0 \coloneqq \gamma(0) = \mu_{\rm C}(t_0)/\mu_{\rm P}(t_0) = \mu_{\rm C,0}/\mu_{\rm P,0}$ as a parameter. From Eqs. (20) and (38) one calculates that

$$\mu_{\rm C,0} + \bar{\mu}_{\rm C,0} = -\frac{3H_0^2}{4\pi\kappa}\,\Omega_{\rm C} . \tag{68}$$

This, together with Eq. (67) and the stipulation that $\bar{\mu}_{\rm P,0}/\mu_{\rm P,0} = -2$, implies that

$$\frac{\bar{\mu}_{\rm C,0}}{\mu_{\rm C,0}} = -\left(1 + \frac{2\,\Omega_{\rm C}}{\gamma_0\,\Omega_{\rm P}}\right) . \tag{69}$$

If, as in the case of P-particles, we assume that all the tunnel C-particles have the same mass parameter $m_{\rm C}$ and same size parameter $n_{\rm C}$, then, just as for P-particles, we have that $\bar{\mu}_{\rm C}/\mu_{\rm C}$ is constant and

$$\left(\frac{m_{\rm C}}{n_{\rm C}}\right)^2 = \frac{[\ln(-\bar{\mu}_{\rm C}/\mu_{\rm C})]^2}{[\ln(-\bar{\mu}_{\rm C}/\mu_{\rm C})]^2 + \pi^2} . \tag{70}$$

TABLE III. Computed parameter values for continuously created C-matter: $\mu_{\rm C}$ (attractive mass density), $m_{\rm C}$ (attractive mass of a particle), $\bar{\mu}_{\rm C}/\mu_{\rm C}$ (ratio of repulsive mass density to attractive mass density), and $\mu_{\rm C}/m_{\rm C}$ (particle number density). Inputs are a selection of assumed values of $r(2\,m_{\rm C})$ (inertial mass of a particle) and γ_0 (ratio at present of attractive mass density of C-matter to that of primordial P-matter, proposed as dark matter to baryonic matter density ratio). The best-fit values $\Omega_{\rm P} = 0.479$ and $\Omega_{\rm C} = 0.954$ are taken from Table II (cf. Table I), with $H_0 = 73.8$ km s^{-1}/Mpc.

Inputs		Outputs			
$r(2\,m_{\rm C})$	$\gamma_0 := \frac{\mu_{\rm C,0}}{\mu_{\rm P,0}}$	$\mu_{\rm C}$ (g/cm^3)	$m_{\rm C}$ (g)	$\frac{\bar{\mu}_{\rm C}}{\mu_{\rm C}}$	$\frac{\mu_{\rm C}}{m_{\rm C}}$ (1/m^3)
$m_{\text{p-n}}$ ($= 1.67 \times 10^{-24}$ g $= 1.24 \times 10^{-52}$ cm)	10	4.90×10^{-29}	1.52×10^{-25}	-1.40	3.23×10^{2}
	100	4.90×10^{-28}	2.04×10^{-26}	-1.04	2.40×10^{4}
	200	9.80×10^{-28}	1.04×10^{-26}	-1.02	9.43×10^{4}
	500	2.45×10^{-27}	4.21×10^{-27}	-1.01	5.82×10^{5}
$10 \times m_{\text{p-n}}$	10	4.90×10^{-29}	1.52×10^{-24}	-1.40	3.23×10^{1}
	100	4.90×10^{-28}	2.04×10^{-25}	-1.04	2.40×10^{3}
	200	9.80×10^{-28}	1.04×10^{-25}	-1.02	9.43×10^{3}
	500	2.45×10^{-27}	4.21×10^{-26}	-1.01	5.82×10^{4}
$10^2 \times m_{\text{p-n}}$	10	4.90×10^{-29}	1.52×10^{-23}	-1.40	3.23×10^{0}
	100	4.90×10^{-28}	2.04×10^{-24}	-1.04	2.40×10^{2}
	200	9.80×10^{-28}	1.04×10^{-24}	-1.02	9.43×10^{2}
	500	2.45×10^{-27}	4.21×10^{-25}	-1.01	5.82×10^{3}
$10^{10} \times m_{\text{p-n}}$	10	4.90×10^{-29}	1.52×10^{-15}	-1.40	3.23×10^{-8}
	100	4.90×10^{-28}	2.04×10^{-16}	-1.04	2.40×10^{-6}
	200	9.80×10^{-28}	1.04×10^{-16}	-1.02	9.43×10^{-6}
	500	2.45×10^{-27}	4.21×10^{-17}	-1.01	5.82×10^{-5}
m_{Planck} ($= 2.18 \times 10^{-5}$ g $= 1.62 \times 10^{-33}$ cm $= 1.31 \times 10^{19} \times m_{\text{p-n}}$)	10	4.90×10^{-29}	1.98×10^{-6}	-1.40	2.48×10^{-17}
	100	4.90×10^{-28}	2.65×10^{-7}	-1.04	1.85×10^{-15}
	200	9.80×10^{-28}	1.35×10^{-7}	-1.02	7.24×10^{-15}
	500	2.45×10^{-27}	5.48×10^{-8}	-1.01	4.47×10^{-14}

Using this equation in conjunction with Eq. (69) and (from Eq. (62)) the equation $n_{\rm C} = r(2\,m_{\rm C})e^{-(m_{\rm C}/n_{\rm C})\alpha(2\,m_{\rm C})}$, we can construct a table of output values of parameters of interest for selected input values of γ_0 and $r(2\,m_{\rm C})$. The result is Table III, which uses $H_0 = 73.8$ km s^{-1}/Mpc and the best-fit values $\Omega_{\rm P} = 0.479$ and $\Omega_{\rm C} = 0.954$ from Table II (cf. Table I).

This discussion has assumed that the mass and size parameters of the P- and C-particles remain constant over time, which need not be the case. Indeed, it is conceivable, perhaps even likely, that these particles would share in the universal contraction and expansion. A particle that did so could be represented by a drainhole model whose choke sphere over the course of time from $-\infty$ to ∞ shrinks from infinitely large to a point, then instantaneously reverses to grow back to infinitely large. Such a model is presented in [32] as a solution of the same field equations that the static drainholes satisfy, namely, Eqs. (7) and (8) with $\mu = \bar{\mu} = 0$ and $\psi = 0$. This model has $m = 0$, thus is devoid of gravity, but it could in principle be modified to one that has $m \neq 0$ (perhaps with the bonus that the choke sphere shrinks to, then expands from, a sphere of minimal radius instead of a point). Allowing the P- and C-particles to contract and expand with the universe would, of course, necessitate a revision of the discussion above and of Table III.

VII. ISSUES AND OBSERVATIONS

The conceptual basis of the model of the cosmos developed in the preceding sections differs in many respects from that of the concordance model. These differences and their consequences bring up a number of issues, some of which have been discussed above to greater or lesser extent, others of which have been passed over. In this section I shall specify and comment on those that I have been able to identify along the way, in approximately the order in which they appeared. For ease of reference I shall call my model the PCB model, and the concordance model the ΛCDM model.

A. Gravity and passive-inertial mass

As noted at the beginning, Newton's law of action and reaction allows the inference that the ratio $m_{\text{ac}}/m_{\text{pa-in}}$ of active gravitational mass to passive-inertial mass is the same for all 'bodies', that is, for all matter in bulk. Because Newton's theory describes gravity as well as it does, this inference must be at least approximately correct. Even if exact, however, it is only a statement about a numerical ratio of quantities that *conceptually* have nothing to do with one another: the generation of a gravitational field on the one hand, the resistance to being accelerated by a field of any sort on the other. To try to force a marriage between these concepts is akin to the proverbial task of trying to fit a square peg into a round hole. If one were to treat this unlikely union as legitimate, then one would have to say that a gravitating body flying by at speed v would have its active gravitational mass and therefore its gravity increased by a factor $1/\sqrt{1-v^2/c^2}$ because that's what happens to its inertial mass. But the 'increase of inertial mass' by that factor has nothing to do with an innate property of the body such as the strength of its gravity or its true inertial mass (i. e., its rest mass m_0 as opposed to its relativistic mass $m_0/\sqrt{1-v^2/c^2}$), rather is simply a quantification of the fact that the closer any body's speed is to the speed of light, the harder it is to make that body go faster when the force field you're using can't propagate faster than light. (The analogy of a person on foot pushing a dead-battery car to get it started is useful: the nearer the car's speed is to the pusher's maximum foot speed, the less able is the pusher to accelerate the car, though the car's inertial mass has not changed.) And let us note in passing that when the shape of the electromagnetic field of an electrically charged particle in uniform motion is observed to depend on the velocity of the particle, this is attributed to the fact that the field propagates at finite speed, not to a change in the particle's electric charge.

If passive-inertial mass is not a source of gravity, then as said in Sec. III Einstein's 'energy-tensor of matter' $T^{\alpha\beta} := \rho u^\alpha u^\beta - (p/c^2)g^{\alpha\beta}$ (consequently, also the 'equation of state') has no role to play in the field equations of gravity, so one loses the alluring implication that $T_\alpha{}^\beta{}_{:\beta} = 0$, which implication Einstein interpreted as saying that a consequence of his field equations was that "the equations of conservation of momentum and energy... hold good for the components of the total energy", and cited as "the strongest reason for the choice" of his equations ([5],§16). The loss of this implication does not, of course, keep us from asserting that $T_\alpha{}^\beta{}_{:\beta} = 0$; it only requires that we look elsewhere for a justification. But one must recognize that for $T_\alpha{}^\beta{}_{:\beta} = 0$, however arrived at, to be interpreted as a proposition about conservation of momentum and energy ρ must be the density of inertial mass, not, as Einstein assumed, the density of active gravitational mass.

All too frequently there appear in the popular press accounts of astronomers 'weighing' the universe or 'weighing' a galaxy. One can object, of course, to the presumably intentional blurring of the distinction between inertial mass and weight, but a larger objection is that such accounts leave the reader with the false impression that determining an entity's active gravitational mass is known to be equivalent to determining its passive-inertial mass (and therefore its weight). Only if one can prove the existence of a universal proportionality between the two can one legitimately claim to have 'weighed' the universe or a galaxy, and even then only indirectly. Unless and until there is such a proof, pretending that the universe or a galaxy has been weighed spreads ignorance, not knowledge. The most elementary unit of knowledge is a distinction made — a fact built into every digital computer. Conversely, the most elementary unit of ignorance is a distinction not made.

B. Choice of a variational principle for gravity

The step up in Sec. III from the nonrelativistic variational principle $\delta\int(|\nabla\phi|^2 + 8\pi\kappa\mu\phi)\,d^3x = 0$ that generates the Poisson equation $\nabla^2\phi = 4\pi\kappa\mu$ to the relativistic principle $\delta\int(\boldsymbol{R} - \frac{8\pi\kappa}{c^2}\mu)\,|g|^{\frac{1}{2}}d^4x = 0$ that generates the equations $\boldsymbol{R}_{\alpha\beta} - \frac{1}{2}\boldsymbol{R}\,g_{\alpha\beta} = -\frac{4\pi\kappa}{c^2}\mu g_{\alpha\beta}$ is an application of Occam's razor, and as such can only be justified retrospectively, by its consequences. Alone, this principle has, through its Euler-Lagrange equations, little to say about cosmology, but when modified by inclusion of the cosmological constant Λ it says something significant, namely, that there is

gravitationally repulsive matter in the universe (disguised as $-\Lambda$), and there's more of it than there is of attractive matter. This is a consequence that has consequences, but to get them all requires the next step up, to the action integrand of Eq. (6) which has in it in addition to the positive and negative mass densities μ and $\bar{\mu}$ the (gradients of the) scalar fields ϕ and ψ, which are considered as auxiliary 'relaxants' not to be varied. What justifies their inclusion?

A defect of the Einstein vacuum field equations, generally unrecognized as such, is that they produce as their basic model for a gravitating particle, namely, the Schwarzschild solution, a manifold that exhibits no *spatial* curvature when viewed from the perspective of a free-falling observer. (This is seen in Eq. (60), in which t is the proper time of free-falling observers and on t = constant cross sections, because $r(\rho) = \rho$, the metric is that of (flat) euclidean 3-space.) Inclusion of the scalar field ϕ in the action integral of Eq. (6) corrects this defect, as it allows the constant-t cross sections of the drainhole model to have the negative spatial curvatures characteristic of the drainhole, and therefore admits the possibility that the space we reside in is something other than euclidean 3-space.

The inclusion of a second scalar field ψ, coupled to the metric with polarity opposite to that of ϕ's coupling, is dictated in the first instance by the absence, when Einstein's assumption of equivalence between passive-inertial mass and active gravitational mass is denied, of any real reason to choose one polarity over the other. In the second instance it is dictated by the observation that, although the presence of ϕ but not of ψ was required for the derivation of the drainhole model, in the construction of the cosmological model absence of ψ would entail absence from Eq. (21) of the $\dot{\beta}^2$ term, in which case Eq. (21) would turn from true to false once $R(t)$ surpassed $\sqrt[3]{B/A_{\rm P}}$ (which is $R_{H_{\rm max}}$ when $k = 0$). Moreover, if the shoe were on the other foot and the $\dot{\alpha}^2$ term were absent, then Eq. (21) would be false when $R(t)$ was less than $\sqrt[3]{B/A_{\rm P}}$. Thus both ϕ and ψ are needed, coupled to the geometry with opposite polarities. One notices that α and β, appearing only in the combination $\dot{\alpha}^2 - \dot{\beta}^2$, can be individuated only by an arbitrary allocation of the righthand side of Eq. (21) that preserves positives and negatives, such as $\dot{\alpha}^2 = c^2 B/R^6 + p$ and $\dot{\beta}^2 = c^2 A_{\rm P} R^3/R^6 + p$, where p is a nonnegative function. This is analogous to the arbitrariness encountered in 'fixing the mix' of densities in Sec. VI.B, and is consistent with the treatment of the densities and the scalar fields as relaxants of the field equations.

That the combination $2\,\phi^{\cdot\gamma}\phi_{.\gamma} - 2\,\psi^{\cdot\gamma}\psi_{.\gamma}$ in the action integrand of Eq. (6) is the real part of $2\,\chi^{\cdot\gamma}\chi_{.\gamma}$, where $\chi := \phi + i\psi$, suggests that space-time as seen here might be a restriction of a more general, at least partly complexified space-time geometry.

C. Inflation and the 'big bounce'

Further evidence that generation of a realistic cosmological model depends on inclusion of the scalar field ϕ with the so-called 'ghost' or 'phantom' coupling to geometry comes from the recognition that without it there is a 'bang' at $R_{\rm min} = 0$ and no inflation to follow, whereas with it there is a bounce at $R_{\rm min} > 0$, followed by inflation. As is evident from the definition of $P_1(R)$ in Eq. (24), as well as from examining Fig. 1, for $R_{\rm min}$ to be positive it is necessary and sufficient that the integration constant B be positive (otherwise $P_1(0) = -B \geq 0$, which would make $R_{\rm min} = 0$). Also evident is that the smaller a positive B is, the closer $R_{\rm min}$ is to 0; in fact, as noted in Sec. IV, $R_{\rm min} \sim \sqrt[3]{B/2A_{\rm P}}$ as $B \to 0$. Moreover, it is clear that the term $2B/3R^6$ in Eq. (23) is the term that produces rapid inflation when R is small by making $\ddot{R}$ large, but only when $B > 0$. And because $B - A_{\rm P}R^3 \sim B - A_{\rm P}(B/2A_{\rm P}) = B/2$ as $B \to 0$, positivity of B demands that the $\dot{\alpha}^2$ term be present in Eq. (21), thus that the scalar field ϕ be present in the field equations, coupled to the space-time geometry with the unconventional polarity. Let us note, moreover, that here there is no mention of a 'slow roll down a potential', a common element in many proposed inflationary scenarios involving an 'inflaton' scalar field. Indeed, that ϕ is treated merely as an aid in describing the space-time geometry rather than as a 'physical source' of the geometry makes the notion of introducing a potential function for ϕ irrelevant.

D. The PCB model vis-à-vis the ΛCDM model

After the matching $-(\mu_{\rm P,0} + \bar{\mu}_{\rm P,0}) = \mu_{\rm M} = \mu_{\rm P,0}$ in Sec. VI.B the only functional difference between the expressions for H^2 in the PCB model and in the ΛCDM model lies in their terms of highest order in $1/\tilde{R}$: $H_0^2\,\Omega_{\rm B}/\tilde{R}^6$ in Eq. (64) and $H_0^2\,\Omega_{\rm R}/\tilde{R}^4$ in Eq. (65). In fully normalized form these equations read

$$H^2 = H_0^2 \left(\Omega_{\rm C} + \Omega_{\rm k} \frac{1}{\tilde{R}^2} + \Omega_{\rm P} \frac{1}{\tilde{R}^3} + \Omega_{\rm B} \frac{1}{\tilde{R}^6} \right) \tag{71}$$

(which is Eq. (42)) and

$$H^2 = H_0^2 \left(\Omega_{\Lambda} + \Omega_{\rm k} \frac{1}{\tilde{R}^2} + \Omega_{\rm M} \frac{1}{\tilde{R}^3} + \Omega_{\rm R} \frac{1}{\tilde{R}^4} \right) . \tag{72}$$

Absent their highest-order terms, and with the obvious identifications among the remaining Ωs, these equations would produce, by way of the corresponding formulas for the distance modulus $\boldsymbol{\mu}$, exactly the same best fits to the SNe Ia data, the parameters and the $\chi^2_{\rm red}$ statistic being those of Table I. The rationale behind the construction of Table II was that, because the SNe Ia data extend into the past only to $z = 1.755$, restoring the $\Omega_{\rm B}$ term in Eq. (71) while retaining the $\Omega_{\rm B} = 0$ best-fit values of the other parameters will yield a fit with negligibly different $\chi^2_{\rm red}$. The same reasoning could be expected to apply also to restoring the $\Omega_{\rm R}$ term in Eq. (72). Indeed, application of Mathematica's NonlinearModelFit to the ΛCDM model with $\Omega_{\rm R}$ constrained by $0 < \Omega_{\rm R} \leq 10^{-4}$ produces best fits with $\Omega_{\rm R} = 10^{-4}$ (excepting $\Omega_{\rm R} = 6 \times 10^{-16}$ for $H_0 = 73.8$, $k = 1$, and 5×10^{-5} for $H_0 = 76.2$, $k = 1$) and the values of Ω_Λ ($\leftarrow \Omega_{\rm C}$), $\Omega_{\rm M}$ ($\leftarrow \Omega_{\rm P}$), $\chi^2_{\rm red}$, t_0, and $z_{\rm a}$ differing from those of Tables I and II by insignificant amounts. It is therefore the case that the PCB model is at least as consistent with the SNe Ia data as the ΛCDM model is. Moreover, the PCB model is singularity-free and includes both a bounce and an inflationary epoch, thus models phenomena that ΛCDM is incapable of modeling (so long as $\Omega_{\rm R} < 0$ is ruled out).

The omission from the PCB-model field equations of a radiation term proportional to $1/R^4$ goes against conventional wisdom but is not without motivation. Inclusion of such a term would seem to violate the basic working hypothesis that energy is not a generator of gravity. Radiant energy, however, although convertible to kinetic energy through its influence on the motion of electrically charged objects, is not kinetic energy and therefore might be a gravity generator. This would presumably come about through a coupling of the electromagnetic field components $F_{\alpha\beta}$ to the space-time geometry. The difficulty is that the usual method of coupling by inserting a term proportional to $F^\gamma{}_\delta F^\delta{}_\gamma$ into the integrand of the action integral has no immediate geometrical justification and produces field equations of the sort that Einstein likened to a building with one wing made of fine marble ($\boldsymbol{R}_{\alpha\beta} - \frac{1}{2}\boldsymbol{R}\, g_{\alpha\beta}$), the other, of low grade wood (e. g., the energy-momentum tensor for F) [33]. What is needed is a version of the PCB model developed in the context of a geometrical unified field theory of the sort that Einstein spent his later years in an unsuccessful quest for. Although I have been able to construct such a theory as a hybrid of Weyl's conformal theory and Kaluza's five-dimensional theory [34], the manner in which that theory's variational principle and field equations connect the electromagnetic field to geometry does not suggest a way to relate F to the space-time geometry in the present context. For this reason I have chosen to omit the radiation term from the field equations governing the PCB model. Such a term can, of course, be reinstated on an *ad hoc* basis if a sufficiently compelling reason for doing so presents itself. Even if, however, radiation were included at the $\Omega_{\rm R} \leq 10^{-4}$ level, the best-fit value $t_0 = 12.52$ Gyr for the PCB model would carry over to the ΛCDM model, which allows the conclusion that the SNe Ia data do not support the commonly quoted value of 13.7 Gyr for the age of the universe.

E. Dark matter, dark 'energy', and the 'Cosmological Constant Problem'

In the ΛCDM model dark matter is lumped with baryonic matter in $\Omega_{\rm M}$ as primordial matter whose density is proportional to $1/R^3$. The unseen, unknown stuff in Ω_Λ, whose density has no R dependence, is called dark 'energy' in compliance with Einstein's assumption that energy is a source of gravity. In the PCB model only baryonic matter is treated as belonging to the primordial $\Omega_{\rm P}$ sector with $1/R^3$ density dependence, dark matter being shifted to the $\Omega_{\rm C}$ sector with density kept constant by continuous creation of the dark C-matter. And there, instead of dark 'energy' represented by a cosmological constant Λ many orders of magnitude too small to be consistent with various origins proposed for this energy, one finds the gravitationally attractive dark matter particles accompanied by their gravitationally repulsive back sides, their net effect represented by the constant $A_{\rm C}$ of Eq. (20), functionally equivalent to Λ and of the requisite smallness. This interpretation of 'dark energy' as the back side of dark matter provides a self-consistent solution of the so-called 'Cosmological Constant Problem'.

F. Ratio of dark matter to baryonic matter

Because in the ΛCDM model the densities of dark matter and baryonic matter are both proportional to $1/R^3$, the ratio of their densities is constant in time. Estimates of that ratio obtained from observations of visible structures such as galaxies and galactic clusters and superclusters as they exist at the present epoch in the vicinity of our galaxy are therefore used in studies of the formation of these structures in the distant past. In the PCB model, on the other hand, the dark matter density is held constant through continuous creation of C-particles, so the ratio $\mu_{\rm C}/\mu_{\rm P}$ of dark C-matter density to baryonic P-matter density is proportional to R^3. Consequently, the value of this ratio at the epoch corresponding to redshift z is $\gamma(z) = \gamma_0/(1+z)^3$, where γ_0 is the ratio at present, several possible values of which are included in Table III for comparison purposes. Taking this dependence of the ratio on redshift as real would no doubt influence the outcomes of studies of structure formation.

G. Continuous creation of C-matter tunnels

The stipulation that the net density $\mu_C+\bar{\mu}_C$ of C-matter stay fixed while the universe is expanding requires that the drainhole tunnels considered to be the particles of C-matter come continuously into existence. By what mechanism might this happen? Wheeler's notion of a 'quantum foam' of wormholes popping into and out of existence would not provide a satisfactory explanation, for in order to keep the density constant each newly created tunnel must either remain in existence or else upon dying be multiply replaced by new ones. A more useful idea is that the tunnels arise from the stretching of space as the universe expands. Once started, this would be a regenerative process, each new tunnel causing by its excess of repulsion over attraction additional stretching that would generate additional tunnels. Such a process, moreover, could be expected to produce particles in a given region of space at a rate proportional to the rate of increase of the volume of that region, thus maintaining a constant particle density. If, as was assumed in Sec. VI.B, these particles are all created with the same mass and size parameters m_C and n_C, the net density would be held constant. As to how the process could begin, one looks to the primordial P-matter tunnels, presumed to have always been present, pushing the universe toward expansion. In the postbounce era the C-particles would add their contribution, the ultimate result being an acceleration of the expansion. In the prebounce era the C-particles, abundant in the distant past, would be dying out with the shrinking of space as the universe contracted into the bounce.

If the primordial P-matter has 'always' existed, then the question of what 'caused' it to exist is better left to the philosophers. Conceivably, however, the P-matter tunnels came into existence as dark matter particles the same way the C-matter tunnels did, but in the inflationary space-stretching era after the bounce. Only later would their entrance portals have acquired the decorations that turned them into baryonic matter. The really fundamental unanswered question, though, is how did space and time come to exist. In fact, the question can be reduced to the existence of space alone, for the Kaluza–Weyl theory described in [34] is based on a construction that produces time (thus space-time) from three-dimensional space and, repeated, produces a secondary time (thus space-time–time) from space-time. And at the space-time stage of that theory there occurs naturally a model of an expanding drainhole in an expanding universe which repels on the low side more strongly than it attracts on the high side and needs no auxiliary scalar field for its description [35].

That all the C-particles are created with the same mass and size parameters is only a convenient assumption. If this assumption is wrong, then the densities μ_C and $\bar{\mu}_C$ might vary, in which case the proportionality of $\mu_C + \bar{\mu}_C$ to $1/R^3$ could cease to be exact. This variability could then be used in an *ad hoc* way to produce some of the putative behaviors that proposed modifications of the ΛCDM model put forth under the rubric 'quintessence' are intended to allow.

It cannot be ruled out that some C-particles (and some P-particles as well) have active gravitational mass $m = 0$, but, because $n \neq 0$, have nonzero inertial mass. Being without electric charge, and possessing some rotational properties as suggested in [28] to be possible, such tunnel particles might be produced in abundance and could serve as models for the ubiquitous cosmic neutrinos. If such models are realistic, then analyses that use cosmological observations to put upper bounds on the neutrino mass scale (the analysis in [36] using observations of galaxy clustering, for example) say nothing about the inertial masses of neutrinos, instead 'constrain' only their active gravitational masses, already assumed in the models to be zero. Even if these models are not realistic, in the absence of any demonstrable relation for neutrinos between the two kinds of mass such analyses based on gravitational effects cannot be presumed to constrain their inertial masses.

One other possibility to consider is that as time goes on a fraction of the C-particles acquire the trappings of baryons and are then able to join in the formation of visible-matter structures. This would offer a way for the universe to avoid a cold, dark ending to its exponentially accelerating expansion.

H. Voids, walls, filaments, and nodes

The PCB model, just as the ΛCDM model, treats matter as uniformly distributed in space, an apparently reasonable assumption on a large enough scale. Observationally, however, a major fraction of space appears to comprise voids nearly empty of matter, separated by walls, filaments, and nodes in which resides most of the matter, both the dark and the visible (baryonic). The formation of this cellular structure is generally considered to be an evolutionary product of early small fluctuations in the density of primordial matter. Explanations along that line are attempts to realize what Peebles has called his "perhaps desperate idea . . . that the voids have been emptied by the growth of holes in the mass distribution" [37]. If besides matter that attracts gravitationally there is also repulsive matter, then that idea can be reinterpreted and the desperation perhaps alleviated, by the simple observation that, whereas attractive matter wants to congregate, repulsive matter is reclusive, pushing all matter, attractive or repulsive, away from itself.

In the PCB model each tunnel particle would presumably be created with its entrance and its exit close to one another in the ambient space. In the ambient space the entrance would attract the exit, but the exit would repel the entrance more strongly, so the two portals would drift apart. Apply this to a multitude of such particles and you might expect to see the exits spread themselves over regions from which they had expelled the entrances, regions therefore devoid of ordinary (i. e., attractive) matter. The entrances, on the other hand, being brought together by both their mutual attractions and the repulsion from the exits, would aggregate into walls, filaments, and nodes on the boundaries between the void regions, just as is seen in the real universe. What is more, the walls, filaments, and nodes so created would likely be, in agreement with observation, more compacted than they would have been if formed by gravitational attraction alone, for the repulsive matter in the voids would increase the compaction by pushing in on the clumps of attractive matter from many directions with a nonkinetic, positive pressure *produced by* repulsive gravity, a pressure not to be confused with the negative pseudo-pressure conjectured in the confines of Einstein's assumption to be a *producer of* repulsive gravity. In this way the PCB model can explain qualitatively the observed cellular structure of the universe with minimal reliance on preexisting fluctuations in the primordial matter density — it is conceivable that creation of tunnel entrance-exit pairs at random locations in random orientations during the inflationary phase would provide in and of itself all the density fluctuations needed to initiate the formation of the voids, walls, filaments, and nodes as they are seen today.

I. Geometric units and inertial mass

In Sec. VI.B, in order to populate Table III, the minimum radius $r(2\,m_{\rm C})$ of the C-particle throats was set equal to various multiples of the proton-neutron inertial mass $m_{\rm p\text{-}n}$, converted to geometric units to give the radius its requisite units of length. Because the conversion from inertial mass units to geometric units ($1\ {\rm g} \rightarrow G/c^2 \times 1\ {\rm g} \approx 7.426 \times 10^{-29}$ cm) involves Newton's gravitational constant G, such a conversion would seem to be at odds with the assumption that inertial mass does not generate gravity. The resolution of this apparent inconsistency, dictated by the proposition that everything that exists is one or another aspect of the geometry of the universe, is that the gram is an artificial unit of inertial mass used for convenience, and that the proper unit of inertial mass is a length, 7.426×10^{-29} cm, for example. That necessitates that $G/c^2 = 1$. The 'geometry is all' proposition dictates also that the second must be considered an artificial unit standing in for a length unit. Taking that unit to be the light-second makes $c = 1$ and, consequently, $G = 1$, which equations are commonly taken as the defining equations of geometric units. Considering the proper units of inertial mass and time to be units of length does not, of course, prevent the use of the gram and the second in their customary contexts.

J. Protons, neutrons, and WIMPs as drainholes

The cosmological model developed in Secs. IV and V and fitted to the SNe Ia data rested on the assumption that the active gravitational mass densities of primordial matter and continuously created matter are on balance negative. The model did not include (or need to include) a mechanism for producing those imbalances. Subsequently, in Sec. VI.B, I proposed as a mechanism that every elementary particle that gravitates is at its core a physical drainhole, and that the excesses of repulsion over attraction of these drainholes cumulatively produce the overall density imbalances. Among the particles in that category would presumably be counted protons, neutrons, and the weakly interacting massive particles (WIMPs) thought to be the constituents of dark matter. From my perspective the drainhole proposal is simply to modify the conception of every such particle as an entity built around a physical blackhole, by substituting for the blackhole a physical drainhole. Such a substitution seems to me no more radical than replacing a blocked drainpipe of a wash basin with a drainpipe that has no blockage. But one must in the first place recognize that the basin *has* a drainpipe, whether blocked or unblocked. I find it more than a little peculiar that there is discussion about the possibility of the Large Hadron Collider's producing a microscopic blackhole through a collision of two protons, when a straightforward application of Einstein's unvarnished theory of gravity suggests that every proton and every neutron in the collider is already built around a blackhole or a collection of blackholes. Are not gravitating bodies just conglomerates of gravitating particles, each making its own small contribution to the gravity of the whole? And if a particle that gravitates has no gravitational sink such as a blackhole or a drainhole associated with it, then what *is* the source of its gravity?

K. Galactic nuclei as drainholes

If instead of a blackhole at the center of our galaxy there is a drainhole, what might it look like? From afar the behavior of matter and radiation around such a drainhole would not differ in appearance from the behavior of matter and radiation around a blackhole of the same mass and approximately the same size. For both a Schwarzschild blackhole of mass m and a drainhole of mass m the radial equation of motion of a test particle is

$$\frac{d^2\rho}{d\tau^2} = -\frac{c^2 m}{r^2(\rho)} + (\rho - 3m)\left(\frac{d\Omega}{d\tau}\right)^2 , \tag{73}$$

with $r(\rho)$ given by Eq. (62) for the drainhole and $r(\rho) = \rho$ for the blackhole. In both cases τ is the proper time of the test particle. Equation (73) shows that for the drainhole as well as for the blackhole $3m$ is its 'star-grabbing' radius, as any star whose orbit takes it down to $\rho = 3m$ or below will never again have $d\rho/d\tau > 0$. The shared metric of the cross sections of constant t being $d\rho^2 + r^2(\rho)\, d\Omega^2$, the cross sections of the blackhole are euclidean, so the geodesic radius $3m$ of the sphere from which no star can escape is also its areal radius. For the drainhole the situation is different: the areal radius is $r(3m)$, which by increasing the size parameter n can be made as large as you like.

For purely radial motion the acceleration $-c^2 m/r^2(\rho)$ in Eq. (73) is the (nonvectorial) gradient $(c^2 f^2/2)'(\rho)$ of the specific kinetic energy $\frac{1}{2}v^2$ of observers free-falling from rest at $\rho = \infty$. It attains its maximum strength $c^2 m/r^2(2m)$ at the choke sphere of the drainhole throat. A measure of the tidal effects in the radial direction is the tidal gradient, given by

$$s(\rho) := \left(\frac{c^2 f^2}{2}\right)''(\rho) = \frac{2(\rho - 2m)}{(\rho - m)^2 + n^2 - m^2} \cdot \frac{c^2 m}{r^2(\rho)} , \tag{74}$$

which vanishes at the choke sphere and reaches a positive, stretching maximum

$$s_{\max} = s(\rho_+) = \frac{\sqrt{3}}{2n + \sqrt{3}\, m} \cdot \frac{c^2 m}{r^2(\rho_+)} \quad \text{at} \quad \rho_+ = 2m + \frac{n}{\sqrt{3}} , \tag{75}$$

and a negative, compressing minimum

$$s_{\min} = s(\rho_-) = -\frac{\sqrt{3}}{2n - \sqrt{3}\, m} \cdot \frac{c^2 m}{r^2(\rho_-)} \quad \text{at} \quad \rho_- = 2m - \frac{n}{\sqrt{3}} . \tag{76}$$

For a fixed m, $s_{\max}$ is a monotonic function of n, decreasing from

$$\lim_{n \to m} s_{\max} = \frac{3\sqrt{3}\,(2 - \sqrt{3}\,)^2 e^{-(3-\sqrt{3}\,)}}{2} \cdot \frac{c^2}{m^2} \tag{77}$$

to 0, while $s_{\min}$ increases monotonically from

$$\lim_{n \to m} s_{\min} = -\frac{3\sqrt{3}\,(2 + \sqrt{3}\,)^2 e^{-(3+\sqrt{3}\,)}}{2} \cdot \frac{c^2}{m^2} \tag{78}$$

to 0, as n increases from m to ∞.

Observations of stars near the galactic center put the central supermass constraining their motions at $m_{\rm gc} \approx 4.31 \times 10^6 M_\odot = 6.36 \times 10^6$ km [38]. In ordinary units $c^2 m_{\rm gc} = 5.72 \times 10^{17}$ km^3/s^2 and $c^2/m_{\rm gc}^2 = 2.22 \times 10^{-3}$ (km/s^2)/km. Building on these, with the ratio $n/m_{\rm gc}$ as an input parameter, Table IV exhibits the corresponding values of the drainhole areal radius $r(2m_{\rm gc})$, the star capture areal radius $r(3m_{\rm gc})$, the maximum radial acceleration $c^2 m_{\rm gc}/r^2(2m_{\rm gc})$, and the tidal gradients $s_{\max}$ and $s_{\min}$.

Everything that falls into a supermassive blackhole encounters unbounded tidal stretching that strips it of its identity as it approaches and reaches the central singularity, never to be seen again. Falling into a supermassive drainhole small things such as dust particles, gas molecules, and photons (and, as the declining values of $s_{\max}$ and $s_{\min}$ in Table IV suggest, even large things such as stars if the ratio $n/m_{\rm gc}$ is large) can retain their identities and exit the drainhole on the downhill, gravitationally repelling side. This brings the following question: If supermassive drainholes at galactic centers are commonplace, and their exits reside in our (part of the) universe, where should we expect to see those exits, and how might we identify them? In accordance with the notion that the exits of drainhole tunnels tend to isolate themselves by pushing all other matter away, the obvious places to look for them would be in the great voids filled with the exits of dark C-matter tunnels. Presumably they would appear as compact, light-emitting objects surrounded by a halo of outflowing gas, their light intrinsically blueshifted from its journey downward in the

TABLE IV. For a drainhole of size parameter n and mass parameter $m_{\rm gc} \approx 4.31 \times 10^6 M_\odot = 6.36 \times 10^6$ km in geometric units (the current best estimate of the supermass at the center of our galaxy), and a range of values of the ratio $n/m_{\rm gc}$, this table exhibits the corresponding values of the drainhole areal radius $r(2m_{\rm gc})$, the star capture areal radius $r(3m_{\rm gc})$, the maximum radial acceleration $c^2 m_{\rm gc}/r^2(2m_{\rm gc})$, and the maximum and minimum tidal gradients $s_{\rm max}$ and $s_{\rm min}$.

Inputs	Outputs				
$\frac{n}{m_{\rm gc}}$	$r(2m_{\rm gc})$ (km)	$r(3m_{\rm gc})$ (km)	$\frac{c^2 m_{\rm gc}}{r^2(2m_{\rm gc})}$ (km s^{-2})	$s_{\rm max}$ (km s^{-2}/km)	$s_{\rm min}$ (km s^{-2}/km)
1	1.73×10^7	2.10×10^7	1.91×10^3	1.16×10^{-4}	-7.07×10^{-4}
10	7.38×10^7	7.41×10^7	1.05×10^2	1.00×10^{-6}	-1.15×10^{-6}
100	6.46×10^8	6.46×10^8	1.37×10^0	1.39×10^{-9}	-1.41×10^{-9}
1000	6.37×10^9	6.37×10^9	1.41×10^{-2}	1.44×10^{-12}	-1.44×10^{-12}
10000	6.37×10^{10}	6.37×10^{10}	1.41×10^{-4}	1.44×10^{-15}	-1.44×10^{-15}
100000	6.36×10^{11}	6.36×10^{11}	1.41×10^{-6}	1.44×10^{-18}	-1.44×10^{-18}

drainholes' gravitational potentials. The brightnesses of such objects would depend on the rate at which the gases and light were sucked into the drainhole entrances. If very bright, they might appear as isolated quasar-like objects. If dim, they might be present in the voids but unseen.

With a little topological imagination one can see how a supermassive drainhole might arise from a plenitude of baryonic P-matter and dark C-matter drainhole tunnels with their entrances brought tightly together by their mutual attractions. Begin with a pair of them, T_1 and T_2 say. If not only their entrances but also their exits were close together, then the coalescing of T_1 and T_2 into a single tunnel might be feasible. If, however, their exits had receded far from one another, then the only way T_1 and T_2 might reasonably coalesce into one tunnel would be to join at their entrances and close off into a single tunnel connecting their original exits. If that occurred, then the 'gravitational ether' flowing into their entrances would be diverted to the nearby entrances of one or more tunnels, thereby increasing their masses, both the attractive and the repulsive. The remnant of T_1 and T_2, no longer connected to the ether flow, would soon become a gravityless tunnel connecting two distant places out in the voids (perhaps, as suggested in Sec. VII.G, manifesting as a neutrino — or a pair of neutrinos). After many repetitions of this process there would be left a single tunnel large enough to accommodate all the combined ether flow of the original P- and C-matter tunnels — a supermassive drainhole.

One can equally well imagine that all the tunnels associated with baryonic matter and dark matter concentrated at a galactic center would retain their identities and their gravity, both the attractive and the repulsive, no matter how tightly packed or rapidly moving their entrances might be. At the tunnel exits there would be nothing new to look for, all the attractive gravity concentrated at their entrances being dispersed in the voids as negative gravity in the same way as it was before the concentration took place. Here there would be no merging of tunnels, thus no altering of the topology of space (and no new creation of neutrinos). Left to be analyzed would be only the simpler changes of spatial topology associated with the creation and destruction of the individual drainhole tunnels.

L. Drainholes and Hawking radiation

Although a drainhole has no horizon capable of producing 'Hawking radiation' by permanently splitting a pair of virtual particles into a member imprisoned inside the horizon and a member escaping as 'radiation', some drainholes can nevertheless perform analogous splittings. Sufficient for this is that the particles arise at a place where the drainhole tidal gradient s is large enough to overcome the binding force between them, which is possible because, according to Eq. (77), $s_{\rm max}$ can be made as large as you like by making m small enough and n close enough to m. After such a separation one member of the pair could be drawn downward into the drainhole while the other escaped upward as outgoing radiation. It should be noted, however, that splitting of pairs of virtual electrons, photons, or neutrinos by a drainhole would not alter the drainhole's mass parameter m (thus could not cause the drainhole to 'evaporate') if the 'devirtualized' particles produce no gravity, as would be consistent with the presumption that Einstein's assumption that energy generates gravity is false.

VIII. SUMMARY

Exploring the consequences of denying Einstein's 1916 assumption that inertial mass and energy are sources of gravity I arrived at the variational principle

$$\delta \int [\boldsymbol{R} - \tfrac{8\pi\kappa}{c^2}(\mu + \bar{\mu}) + 2\,\phi^{\cdot\gamma}\phi_{.\gamma} - 2\,\psi^{\cdot\gamma}\psi_{.\gamma}]\,|g|^{\frac{1}{2}} d^4x = 0,$$

in which ϕ and ψ are scalar fields and μ and $\bar{\mu}$ are the *active* gravitational mass densities of distributions of gravitationally attractive and gravitationally repulsive matter, and in which, to accord with the precept that in a space-time manifold nothing extraneous to the metric should participate in the extremizing of the action, only the space-time metric is varied in deriving the field equations to govern the space-time geometry. This logically consistent, purely geometrical version of Einstein's theory of gravity was then found to be capable of performing feats the original version could not perform. Specifically, the modified version was found to be able to:

- Produce cosmological models that replace the 'big bang' with a 'big bounce', include in their expansion inflation, deceleration, coasting, and ultimate exponential acceleration, and provide good fits to Hubble plots of type Ia supernovae data.
- Solve the 'Cosmological Constant Problem', by identifying $-\frac{c^2}{4\pi\kappa}\Lambda$ as the net active mass density of gravitating matter.
- Replace the Schwarzschild blackhole with a singularity-free, horizonless, topological 'drainhole' that gravitationally attracts matter on its high, front side while gravitationally repelling matter more forcefully on its low, back side.
- Represent dark matter by the attracting entrance portals of drainhole tunnels and dark 'energy' by the repelling exit portals of those tunnels.
- Suggest a new, drainhole-based mechanism for the creation and evolution of cosmic voids, walls, filaments, and nodes.
- Exorcise 'phantoms', 'ghosts', and 'exotic matter' from the body of gravitational physics.

In view of these successes, as well as its logical consistency, one can justifiably consider Einstein's theory of gravity modified in this way to be an improved version of the original.

[1] H. G. Ellis, Ether flow through a drainhole: A particle model in general relativity, *J. Math. Phys.* **14** (1973), 104–118; Errata: **15** (1974), 520; see also Sec. VI.A of the present paper.

[2] K. A. Bronnikov, Scalar-tensor theory and scalar charge, *Acta Phys. Pol.* **B4** (1973), 251–266.

[3] O. Bergmann and R. Leipnik, Space-time structure of a static spherically symmetric scalar field, *Phys. Rev.* **107** (1957), 1157–1161.

[4] A. Einstein, *Essays in Science*, (Philosophical Library, New York, 1934) pp. 98–111.

[5] A. Einstein, Die Grundlage der allgemeinen Relativitätstheorie, *Ann. der Physik* **49** (1916), 769–822, translated in *The Principle of Relativity* (Dover, New York, 1952) pp. 109–164.

[6] G. Galilei, *Dialogues Concerning Two New Sciences* (Prometheus Books, Buffalo, N.Y., 1991) pp. 63 *et seq.*; `http://galileoandeinstein.physics.virginia.edu/tns_draft/index.html` (pp. 63 *et seq.*).

[7] A. Einstein, *Relativity, The Special and the General Theory: A Popular Exposition*, (Methuen, London, 1916), (Bonanza Books, New York, 1961) p. 66; also available as an eBook (Routledge, London, New York, 2002).

[8] D. F. Bartlett and D. Van Buren, Equivalence of active and passive gravitational mass using the moon, *Phys. Rev. Lett.* **57** (1986), 21–24.

[9] L. B. Kreuzer, Experimental measurement of the equivalence of active and passive gravitational mass, *Phys. Rev.* **169** (1968), 1007–1012.

[10] C. S. Unnikrishnan and G. T. Gillies, Do leptons generate gravity? First laboratory constraints obtained from some G experiments and possibility of a new decisive constraint, *Phys. Lett. A* **288** (2001), 161–166.

[11] H. G. Ellis, Leptons might not generate gravity, `gr-qc/0308082v3` (2004); NB second sentence of third footnote might need revising.

[12] H. Bondi, Negative mass in general relativity, *Rev. Mod. Phys.* **29** (1957), 423–428.

[13] D. Hilbert, Die Grundlagen der Physik (Erste Mitteilung), *Nachr. Königl. Gesellschaft d. Wiss. Göttingen, Math.-Phys. Kl.*, 395–407; reprised in *Math. Annalen* **92** (1924), 1–32.
[14] A. Riess, et al., New Hubble Space Telescope discoveries of Type Ia supernovae at $z > 1$: Narrowing constraints on the early behavior of dark energy, *Astrophys. J.* **659** (2007), 98–121.
[15] A. Riess, et al., A 3% solution: Determination of the Hubble constant with the Hubble Space Telescope and Wide Field Camera 3, *Astrophys. J.* **730** (2011), 119: 1–18.
[16] G. Clément, The Ellis Geometry (Letter to the editor), *Am. J. Phys.* **57** (1989), 967.
[17] L. Chetouani and G. Clément, Geometrical-optics in the Ellis geometry, *Gen. Relativ. Gravit.* **16** (1984), 111–119.
[18] G. Clément, Scattering of Klein-Gordon and Maxwell waves by an Ellis geometry, *Int. J. Theor. Phys.* **23** (1984), 335–350.
[19] S. Kar, D. Sahdev, and B. Bhawal, Scalar waves in a wormhole geometry, *Phys. Rev. D* **49** (1994), 853–861.
[20] C. Armendáriz-Picón, On a class of stable, traversable Lorentzian wormholes in classical general relativity, *Phys. Rev. D* **65** (2002), 104010-1–10.
[21] H. Shinkai and S. A. Hayward, Fate of the first traversible wormhole: Black-hole collapse or inflationary expansion, *Phys. Rev. D* **66** (2002), 044005-1–9.
[22] V. Perlick, Exact gravitational lens equation in spherically symmetric and static spacetimes, *Phys. Rev. D* **69** (2004), 064017-1–10.
[23] A. Das and S. Kar, The Ellis wormhole with 'tachyon matter', *Class. Quantum Grav.* **22** (2005), 3045–3053.
[24] K. K. Nandi, Y-Z. Zhang, and A. V. Zakharov, Gravitational lensing by wormholes, *Phys. Rev. D* **74** (2006), 024020-1–13.
[25] T. Müller, Exact geometric optics in a Morris-Thorne wormhole spacetime, *Phys. Rev. D* **77** (2008), 044043-1–11.
[26] D. K. Dey and S. Sen, Gravitational lensing by wormholes, *Mod. Phys. Lett. A* **23** (2008), 953–962.
[27] A. G. Doroshkevich, N. S. Kardashev, D. I. Novikov, and I. D. Novikov, The passage of radiation through a wormhole, *Astron. Rep.* **52** (2008), 685–691.
[28] T. Matos and D. Nuñez, Rotating scalar field wormhole, *Class. Quantum Grav.* **23** (2006), 4485–4495.
[29] K. K. Nandi, I. Nigmatzyanov, and R. Izmailov, New features of extended wormhole solutions in the scalar field gravity theories, *Class. Quantum Grav.* **25** (2008), 165020-1–19.
[30] A. J. S. Hamilton and J. Lisle, The river model of blackholes, *Am. J. Phys.* **76** (2008), 519–532.
[31] A. Einstein and N. Rosen, The particle problem in the general theory of relativity, *Phys. Rev.* **48** (1935), 73–77.
[32] H. G. Ellis, The evolving, flowless drainhole: A nongravitating particle model in general relativity theory, *Gen. Relativ. Gravit.* **10** (1979), 105–123.
[33] A. Einstein, *Essays in Physics*, (Philosophical Library, New York, 1950) p. 39.
[34] H. G. Ellis, Space-time–time: Five-dimensional Kaluza–Weyl space, `gr-qc/0107023` (2001); Space-time–time, `gr-qc/0205029` (2002).
[35] H. G. Ellis, Darkholes: Nicer than blackholes — with a bright side, too (Does energy produce gravity?), `gr-qc/0003024` (2000).
[36] S. A. Thomas, F. B. Abdalla, and O. Lahav, Upper bound of 0.28 eV on neutrino masses from the largest photometric redshift survey, *Phys. Rev. Lett.* **105** (2010), 031301-1–4.
[37] P. J. E. Peebles, The void phenomenon, *Astrophys. J.* **557** (2001), 495–504.
[38] S. Gillessen, et al., Monitoring stellar orbits around the massive black hole in the galactic center, *Astrophys. J.* **692** (2009), 1075–1109.

Homepage: `http://euclid.colorado.edu/~ellis` Electronic mail: ellis@euclid.colorado.edu